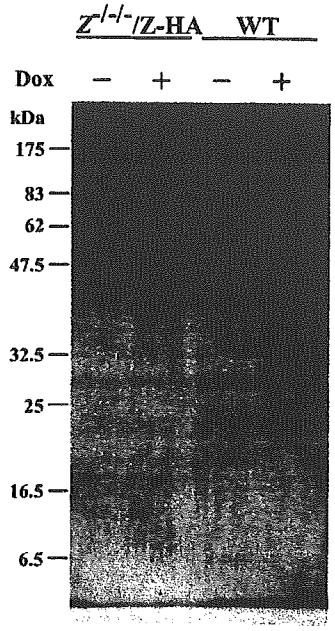

FIG. 4. **Accumulation of poly-ubiquitinated proteins in $Z^{-/-/-}$/Z-HA cells.** The wild-type (*WT*) and $Z^{-/-/-}$/Z-HA cells were treated with (+) or without (−) Dox for 30 h. Cell extracts (10 μg of protein) were subjected to Western blot analysis using an anti-poly-ubiquitin antibody.

precursor Z-HA was not observed in fractions 7–11. In addition, very low mature Z-HA was recovered near top fractions 1–5, which might be generated by disassembly of the 20 S proteasome.

The peptidase activities in fractions of the mature form of Z-HA were high in untreated cells, whereas they were markedly low in Dox-treated cells fractionated in the same manner (Fig. 3, *upper panels*). Taken together, these results suggest that Z-HA is functionally active and that proteasome activity is dependent on the expression of Z-HA. Because not only trypsin-like activity but also other peptidase activities were affected by loss of Z-HA, we concluded that the integral functions of the proteasome are impaired probably due to its inappropriate assembly and/or maintenance of the complex.

Accumulation of Poly-ubiquitinated Proteins Associated with Loss of Z—In the next experiment, we analyzed the levels of cellular poly-ubiquitinated proteins after Z depletion. After wild-type DT40 and $Z^{-/-/-}$/Z-HA cells had been treated with Dox for 30 h, these cell extracts were analyzed by Western blotting using an anti-poly-ubiquitin antibody. As shown in Fig. 4, poly-ubiquitinated proteins considerably increased in crude extracts from the $Z^{-/-/-}$/Z-HA cells by Dox treatment, whereas the pattern of poly-ubiquitinated proteins remained unchanged in wild-type cells, irrespective of Dox treatment. These results suggested that the dysfunction of proteasomes leads to accumulation of poly-ubiquitinated proteins.

Z Subunit Is Essential for Viability—Because most of the proteasome subunit is essential in yeast, we tested the effect of loss of proteasome function on cell viability of $Z^{-/-/-}$/Z-HA cells. For this purpose, $Z^{-/-/-}$/Z-HA cells were treated with Dox for the indicated times and their viability was measured (Fig. 5*A*). Dox-treated $Z^{-/-/-}$/Z-HA cells proliferated in the first 24 h but began to decrease from 30 h of treatment. Flow cytometric analysis of these cells showed their arrest at G_2/M phase (Fig. 5*B*). We next examined the expression of Wee1 kinase, which plays a role in checkpoint mechanism at G_2/M phase (21). Considerable accumulation of Wee1 kinase was noted at 24 h after Dox treatment (Fig. 5*C*). Furthermore, flow cytometry revealed cell death at 30 h after Dox treatment (Fig. 5*B*). To examine whether this was due to apoptosis, we performed TUNEL analysis (Fig. 5*D*). The apoptotic cells had large nuclei and less Z-HA expression. Taken together, these results indicated that loss of Z-HA and proteasomal activities result in cell-cycle arrest at G_2/M phase followed by cell death. It is worth noting that residual Z-HA was present mainly in the cytoplasm as a punctate-like structure and to a lesser extent in the nuclei of Dox-treated cells, whereas it was uniformly present in the cytoplasm and rather abundantly in the nuclei of untreated cells (Fig. 5*D*).

Enhanced Expression of Hsp70 and Hsp40 in Proteasome-defective Cells—It is known that damaged proteins and/or misfolded proteins are rapidly eliminated from the cells by the ubiquitin-proteasome system. Indeed, proteasome inhibitors induce accumulation of such abnormal proteins in the cells and trigger signals that up-regulate the expression of certain molecular chaperones in the cells (22). Given that the expression of proteasomes can be reduced in $Z^{-/-/-}$/Z-HA cells, we next examined whether Z depletion could up-regulate the expressions of major molecular chaperones, Hsp40 and Hsp70 in $Z^{-/-/-}$/Z-HA cells. As shown in Fig. 6 (*lower panels*), Hsp40 and Hsp70 were consistently up-regulated by Z depletion in $Z^{-/-/-}$/Z-HA cells. In contrast, these effects were not observed in Dox-treated wild-type DT40 cells (Fig. 6, *upper panels*). These results suggested that these molecular chaperones are up-regulated upon loss of proteasome function.

DISCUSSION

The proteasome is a multifunctional protease complex and essential for cell viability. We generated $Z^{-/-/-}$/Z-HA cell line in which the expression of proteasome subunit Z could be manipulated by Dox. This cell line expressed Dox-repressible Z protein, tagged with C-terminal HA peptide. The C-terminal HA-tag did not interfere with the wild-type function of Z, because (i) Z-HA complemented the lethality of Z null-phenotype (Fig. 5*A*) and (ii) Z-HA was processed in mature form and incorporated into the proteasome complex (Figs. 1*D* and 3). Depletion of Z-HA resulted in inhibition of three types of proteasomal peptidase activities and ODC-degrading activity (Figs. 2 and 3). Furthermore, considerable accumulation of poly-ubiquitinated cellular proteins was observed *in vivo* (Fig. 4). This is consistent with the fact that cellular poly-ubiquitinated proteins accumulate in the yeast proteasomal temperature-sensitive mutants under restrictive temperature (23). Taken together, these results suggest that the Z subunit is essential for the integrity of proteasome.

The proteasome is the major protease for poly-ubiquitinated proteins and known to degrade many cell-cycle regulators during the cell cycle progression. Most of the yeast proteasome subunit mutants, although not all, exhibit cell-cycle arrest at the G_2/M phase rather than the G_1/S phase (24). Our data also indicate that the major function of the proteasome in cell-cycle regulation is required at the G_2/M phase rather than the G_1/S phase. The essential substrates to be degraded by the proteasome at G_2/M phase were not characterized in this study; however, we observed accumulation of Wee1 kinase in Z-HA knockdown cells (Fig. 5*C*). The Wee1 kinase is known to phosphorylate cyclin-dependent kinase 1 and thus plays a critical role in the checkpoint mechanism by inhibiting cyclin-dependent kinase 1 activity (21). Whether Wee1 kinase is one of the essential substrates or simply accumulates due to cell-cycle arrest at G_2/M phase remains to be elucidated.

The ubiquitin-proteasome system has been implicated in quality control of proteins in the cytosol and endoplasmic reticulum (ER). Accumulation of unfolded proteins in the ER induces the unfolded protein response (UPR), which (i) halts

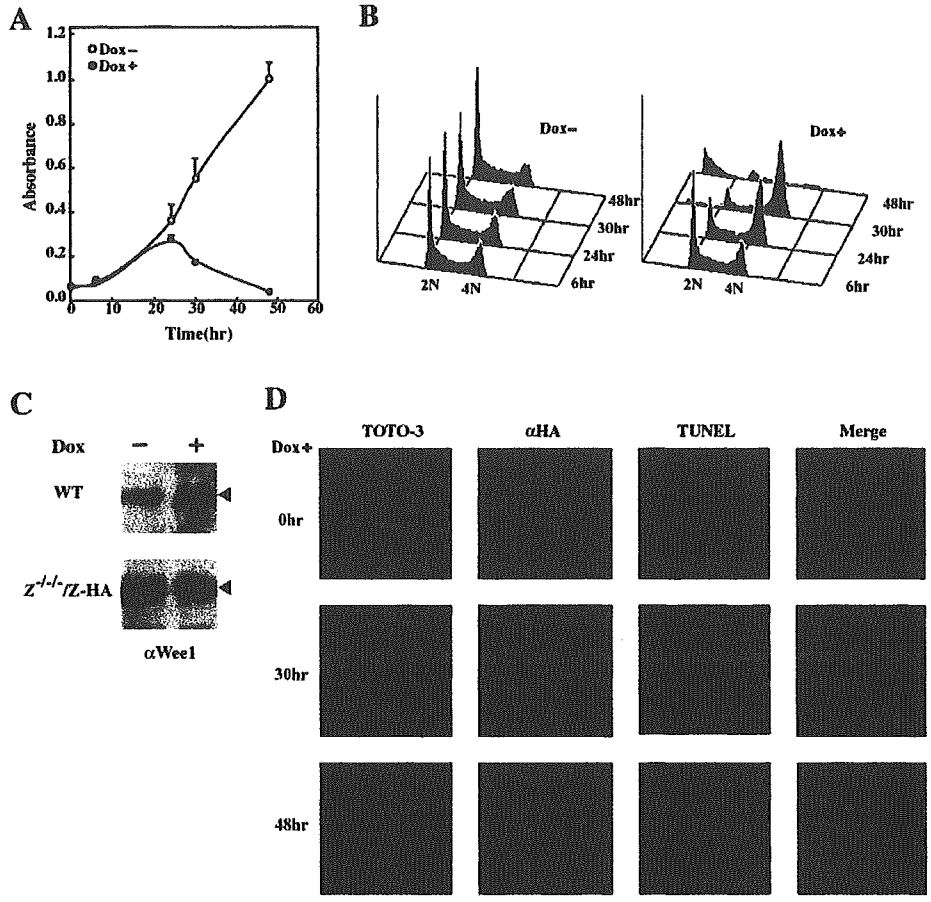

FIG. 5. **The Z subunit is essential for cell viability.** *A*, cell survival after Dox treatment. $Z^{-/-/-}$/Z-HA cells (2×10^4cells) were cultured in the presence (*solid circles*) or absence (*open circles*) of Dox for indicated times (0, 6, 24, 30, and 48 h), and their viabilities were measured. Data represent the mean ± S.D. values of four independent analyses. *B*, cell cycle analysis. Cells were treated as in *A* and subjected to flow cytometric analyses. *Left panel*, Dox-untreated $Z^{-/-/-}$/Z-HA cells; *right panel*, Dox-treated $Z^{-/-/-}$/Z-HA cells. Displayed data show typical patterns, and essentially similar results were obtained in at least three independent experiments. *C*, increment of Wee1 in Z-depleted cells. The crude extracts (20 μg of protein), prepared from wild-type (*WT*) (*upper panels*) and $Z^{-/-/-}$/Z-HA (*lower panels*) cells that had been cultured with or without Dox for 24 h were immunoblotted with anti-Wee1 antibody. *D*, immunofluorescence analysis. Cells were treated as in *A* for the indicated times (0, 30, and 48 h) and mounted onto slides, fixed, and stained. DNA stain (TOTO-3, *blue*), the expression of Z-HA (αHA, *red*), and apoptotic signals (TUNEL, *green*), in the same cells are shown together with the merged images (*Merge*).

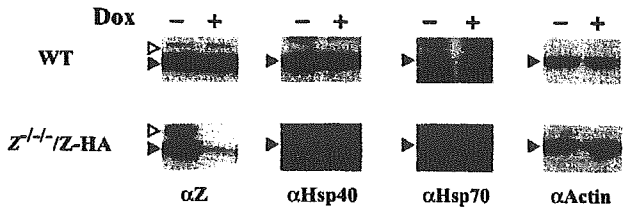

FIG. 6. **Enhanced expression of molecular chaperones Hsp70 and Hsp40 in Dox-treated $Z^{-/-/-}$/Z-HA cells.** Wild-type (*WT*) (*upper panels*) and $Z^{-/-/-}$/Z-HA (*lower panels*) cells were treated with or without Dox for 30 h. Cell extracts (10 μg of protein) were prepared and used for immunoblotting with antibodies against Z, Hsp40, Hsp70, and actin. The *solid arrowheads* indicate the respective proteins, whereas *open arrowheads* show the precursor form of Z.

the translation of newly synthesized proteins, (ii) enhances the expression of molecular chaperones, and (iii) back translocates unfolded protein in the ER to the cytosol for proteasome degradation (25). The last process is called ER-associated protein degradation among the UPR reactions (26). In the present study, our results showed that inhibition of the proteasome enhances the expression of Hsp70 and Hsp40. The latter is known to collaborate with the former for folding newly synthesized and damaged proteins (27). How the cells sense the level of the proteasome and induce these molecular chaperones is unknown at present. However, this process is most likely due to enhanced UPR, because failure of protein degradation results in accumulation of abnormal proteins. Furthermore, the expression of molecular chaperone might be further enhanced following failure of the ER-associated protein degradation pathway.

Ubiquitin and proteasome-dependent protein degradation play essential roles in various biological events as mentioned in the introduction. In this regard, recent studies in the ubiquitin field reveal novel functions for ubiquitin in various biological events such as endocytosis, DNA repair, transcriptional regulation, and kinase activation (28). Whether these events do or do not involve proteasome-dependent degradation remain to be elucidated by genetic means, because proteasome inhibitors are known to inhibit some of the above biological events, such as endocytosis (29). Furthermore, many de-ubiquitinating enzymes that counteract with ubiquitination are vital in the cells (28). Thus, $Z^{-/-/-}$/Z-HA cells could be used as a tool for examining the function of proteasomes in various cellular events that, at least, involve ubiquitination.

Acknowledgments—We thank Y. Yamaguchi-Iwai for providing the parental DT40 cell line, the drug-resistance cassettes, and the pUHD10–3 vector and Y. Murakami for providing ODC and antizyme.

We also thank K. Iwatsuki, T. Yasuda, and all members of the Tanaka laboratory for the advice and technical assistance.

REFERENCES

1. Coux, O., Tanaka, K., and Goldberg, A. L. (1996) *Annu. Rev. Biochem.* **65,** 801–847
2. Baumeister, W., Walz, J., Zuhl, F., and Seemuller, E. (1998) *Cell* **92,** 367–380
3. Groll, M., Ditzel, L., Lowe, J., Stock, D., Bochtler, M., Bartunik, H. D., and Huber, R. (1997) *Nature* **386,** 463–471
4. Unno, M., Mizushima, T., Morimoto, Y., Tomisugi, Y., Tanaka, K., Yasuoka, N., and Tsukihara, T. (2002) *Structure* **10,** 609–618
5. Hershko, A., and Ciechanover, A. (1998) *Annu. Rev. Biochem.* **67,** 425–479
6. Pickart, C. M. (2001) *Annu. Rev. Biochem.* **70,** 503–533
7. Hochstrasser, M. (1997) *Annu. Rev. Genet.* **30,** 405–439
8. Rock, K. L., Gramm, C., Rothstein, L., Clark, K., Stein, R., Dick, L., Hwang, D., and Goldberg, A. L. (1994) *Cell* **78,** 761–771
9. Bogyo, M., McMaster, J. S., Gaczynska, M., Tortorella, D., Goldberg, A. L., and Ploegh, H. (1997) *Proc. Natl. Acad. Sci. U. S. A.* **94,** 6629–6634
10. Fenteany, G., Standaert, R. F., Lane, W. S., Choi, S., Corey, E. J., and Schreiber, S. L. (1995) *Science* **268,** 726–731
11. Kim, K. B., Myung, J., Sin, N., and Crews, C. M. (1999) *Bioorg. Med. Chem. Lett.* **9,** 3335–3340
12. Gossen, M., and Bujard, H. (1992) *Proc. Natl. Acad. Sci. U. S. A.* **89,** 5547–5551
13. Buerstedde, J. M., and Takeda, S. (1991) *Cell* **67,** 179–188
14. Laemmli, U. K. (1970) *Nature* **227,** 680–685
15. Bradford, K. D. (1976) *Anal. Biochem.* **72,** 248–254
16. Tanahashi, N., Murakami, Y., Minami, Y., Shimbara, N., Hendil, K. B., and Tanaka, K. (2000) *J. Biol. Chem.* **275,** 14336–14345
17. Tanaka, K., Yoshimura, T., Kumatori, A., Ichihara, A., Ikai, A., Nishigai, M., Kameyama, K., and Takagi, T. (1988) *J. Biol. Chem.* **263,** 16209–16217
18. Schmidtke, G., Schmidt, M., and Kloetzel, P.-M. (1997) *J. Mol. Biol.* **268,** 95–106
19. Arendt, C. S., and Hochstrasser, M. (1997) *Proc. Natl. Acad. Sci. U. S. A.* **94,** 7156–7161
20. Heinemeyer, W., Fischer, M., Krimmer, T., Stachon, U., and Wolf, D. H. (1997) *J. Biol. Chem.* **272,** 25200–25209
21. Russell, P., and Nurse, P. (1987) *Cell* **49,** 559–567
22. Sherman, M. Y., and Goldberg, A. L. (2001) *Neuron* **29,** 15–32
23. Kominami, K., DeMartino, G. N., Moomaw, C. R., Slaughter, C. A., Shimbara, N., Fujimuro, M., Yokosawa, H., Hisamatsu, H., Tanahashi, N., Shimizu, Y., Tanaka, K., and Toh-e, A. (1995) *EMBO J.* **14,** 3105–3115
24. Ghislain, M., Udvardy, A., and Mann, C. (1993) *Nature* **366,** 358–362
25. Ma, Y., and Hendershot, L. M. (2001) *Cell* **107,** 827–830
26. Plemper, R. K., and Wolf, D. H. (1999) *Trends Biochem. Sci* **24,** 266–270
27. Frydman, J. (2001) *Annu. Rev. Biochem.* **70,** 603–647
28. Weissman, A. M. (2001) *Nat. Rev. Mol. Cell Biol.* **2,** 169–178
29. Longva, K. E., Blystad, F. D., Stang, E., Larsen, A. M., Johannessen, L. E., and Madshus, I. H. (2002) *J. Cell Biol.* **5,** 843–854

The EMBO Journal Vol. 22 No. 14 pp. 3557–3567, 2003

The molecular chaperone Hsp90 plays a role in the assembly and maintenance of the 26S proteasome

Jun Imai[1,2,3], Mikako Maruya[2,3], Hideki Yashiroda[1,3], Ichiro Yahara[3,4] and Keiji Tanaka[1,3,5]

[1]Department of Molecular Oncology and [2]Department of Cell Biology, Tokyo Metropolitan Institute of Medical Science, Honkomagome 3-18-22, Bunkyo-ku, Tokyo 113-8613, [3]CREST, Japan Science and Technology Corporation, Honmachi 4-1-8, Kawaguchi, Saitama 332-0012 and [4]Ina Laboratory, Medical and Biological Laboratories Co. Ltd, 1063-103 Ohara Terasawaoka, Ina, Nagano 396-0002, Japan

[5]Corresponding author
e-mail: tanakak@rinshoken.or.jp

Hsp90 has a diverse array of cellular roles including protein folding, stress response and signal transduction. Herein we report a novel function for Hsp90 in the ATP-dependent assembly of the 26S proteasome. Functional loss of Hsp90 using a temperature-sensitive mutant in yeast caused dissociation of the 26S proteasome. Conversely, these dissociated constituents reassembled in Hsp90-dependent fashion both *in vivo* and *in vitro*; the process required ATP-hydrolysis and was suppressed by the Hsp90 inhibitor geldanamycin. We also found genetic interactions between Hsp90 and several proteasomal Rpn (Regulatory particle non-ATPase subunit) genes, emphasizing the importance of Hsp90 to the integrity of the 26S proteasome. Our results indicate that Hsp90 interacts with the 26S proteasome and plays a principal role in the assembly and maintenance of the 26S proteasome.

Keywords: assembly/Hsp90/maintenance/26S proteasome/yeast

Introduction

The high density of protein molecules in the cytosol increases the likelihood that partially folded or unfolded proteins will undergo off-pathway reactions, such as aggregation, in the protein biosynthetic pathway or by postsynthesis damage. Molecular chaperones recognize proteins with non-native structures, prevent them from irreversible aggregation and assist in their conversion to a functional conformation (Frydman, 2001). On the other hand, the ubiquitin–proteasome pathway plays a pivotal role in selective destruction of misfolded and unassembled proteins (Sherman and Goldberg, 2001). Since chaperones and proteasomes appear to recognize common substrates under non-native states, these two pathways act jointly to prevent aggregation and accumulation of abnormal proteins, thus maintaining protein homeostasis in cells. However, the relationship between molecular chaperones and the ubiquitin–proteasome system is still largely unknown.

Most cellular proteins in eukaryotic cells are targeted for degradation by the 26S proteasome, usually after they have been covalently attached to ubiquitin in the form of a poly-ubiquitin chain functioning as a degradation signal (Pickart, 2001). The 26S proteasome, a eukaryotic ATP-dependent protease, is composed of a catalytic 20S proteasome (alias CP, core particle) and a pair of symmetrically disposed regulatory particles (RP, alias PA700 or the 19S complex) (Baumeister *et al.*, 1998). RP is attached to both ends of the central CP in opposite orientation to form the active 26S proteasome. The 26S proteasome with a molecular mass of ~2.5 MDa acts as a highly organized apparatus for proteolysis. The 20S proteasome is composed of two copies of 14 different subunits, seven distinct α-type and seven distinct β-type subunits. It is a barrel-like particle formed by the axial stacking of four rings made up of two outer α-rings and two inner β-rings, associated in the order αββα. Three β-type subunits of each inner ring have catalytically active threonine residues at their N-termini, and these active sites reside in a chamber formed by the centers of the abutting β-rings. The regulator RP is a protein complex (>700 kDa) composed of ~20 subunits, each 25–110 kDa in size (Baumeister *et al.*, 1998). RP consists of two subcomplexes, known as 'base' and 'lid', which, in the 26S proteasome, correspond to the portions of RP proximal and distal, respectively, to the 20S proteasome (Glickman *et al.*, 1998). The base is mainly composed of up to six ATPases (Rpt, Regulatory particle triple ATPase), while the lid contains multiple non-ATPase subunits (Rpn). The metabolic energy liberated by these Rpt functions is probably utilized for unfolding target proteins so that they can penetrate the channel of the α- and β-rings of the 20S proteasome. However, the roles of many other RP subunits remain undefined.

Of many molecular chaperones, Hsp90 is one of the major species which also requires ATP for its *in vivo* functions (Panaretou *et al.*,1998; Young *et al.*, 2001). It is among the most abundant proteins in cells, occupying ~1–2% of total cellular proteins (Frydman, 2001). The major role of Hsp90 is to manage protein folding, but it also plays a critical role in signal transduction pathways that include mainly steroid receptors and protein kinases (Richter and Buchner, 2001). In *Saccharomyces cerevisiae*, two Hsp90 species with redundant functions, named Hsp82 and Hsc82, are present, which are equivalent to mammalian Hsp90α and Hsp90β, respectively.

In the present study of Hsp90 in the budding yeast, we unexpectedly noticed that *in vivo* inactivation of Hsp90 using the temperature-sensitive (ts$^-$) *hsp82–4Δhsc82* mutant cells (Kimura *et al.*, 1994) caused almost complete dissociation of the 26S proteasome into its constituents. Furthermore, we found that Hsp90 contributes not only to maintain the functional integrity of the 26S proteasome but

also to assist its assembly *in vivo* and *in vitro* in an ATP-dependent manner. In addition, we also provide the genetic evidence of *in vivo* linkage between Hsp90 and the 26S proteasome. Thus the participation of Hsp90 in the 26S proteasome assembly may provide new mechanistic insight into the cooperative interactions between molecular chaperones and proteolysis systems.

Results

Severe thermal stress causes disassembly of the 26S proteasome

To focus on the relationship between stress response and the cellular proteolysis machinery, we examined the effect of severe heat stress on the functional state of the proteasome, which is subclassified into three species in the budding yeast; i.e. the free 20S proteasome (alias CP and here designated simply as C) and RP associated with both sides of CP (R2C) or one side of CP (RC), as described by Glickman *et al.* (1998). Wild-type (WT) cells grown at 25°C were first incubated at 37°C for 1 h. This step was essential to allow the cells to survive a subsequent severe thermal insult. The same cells were incubated at 50°C for 20 min and then shifted to normal culture conditions at 25°C. Upon these stresses, after preconditioning at 37°C, more than 80% of the cells were viable, forming colonies when plated at 25°C (Imai and Yahara, 2000).

Native (non-denaturing) polyacrylamide gel electrophoresis (PAGE) analysis and subsequent western blotting using antibodies against the yeast 20S proteasome

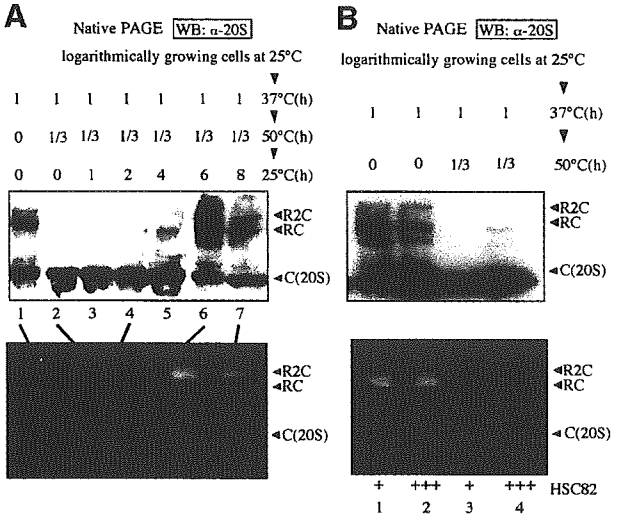

Fig. 1. Dissociation and reassembly of the 26S proteasome after severe heat shock. (**A**) Crude extracts (5 μg) of cells thermally treated as indicated were subjected to native PAGE followed by western blotting (WB) with anti-20S proteasome (top). Cell extracts (20 μg, top, lanes 1, 2, 4, 6 and 7) were loaded onto native PAGE, and thereafter Suc-LLVY-AMC degrading activities were assayed by the in-gel overlay method with 2 mM ATP (bottom). See text for explanation of symbols R2C, RC and C (20S). (**B**) Effect of overexpression (designated as +++) of Hsc82 on the disassembly of the 26S proteasome by severe heat shock. The analyses were similar to those described in (A), except that cells were grown in SC-U medium and cell extracts were prepared from control cells (YPH500/pYO326, lanes 1 and 3) and Hsc82 overexpressing cells (YPH500/pYO326-HSC82, lanes 2 and 4). Note that the magnitude of the increased level by a plasmid overexpressing Hsp82 was more than 5-fold (Imai and Yahara, 2000).

revealed a marked decrease of both the R2C and RC forms of the 26S proteasome after severe heat shock at 50°C, and a considerable increase in the amount of free 20S proteasome (Figure 1A, lanes 2–4). When these heat-shocked cells were reversed to culture at 25°C, it took ~6 h for the full recovery of the 26S proteasome (Figure 1A, lane 6). We also examined the peptidase activity of the 26S proteasome by the in-gel overlay assay. Samples of cell extracts were subjected to native PAGE, and peptide-degrading activity was detected by soaking the gel in a solution containing the fluorogenic peptide succinyl-Leu-Leu-Val-Tyr-7-amino-4-methylcoumarin (Suc-LLVY-AMC). As shown in Figure 1A (bottom), the dissociated 20S proteasome due to severe thermal insults was the latent form and the reassembled 26S proteasome (after incubation at 25°C) was functionally active.

In addition, we found that overexpression of Hsp90 (Hsc82) partially suppressed the destruction of the 26S proteasome caused by severe thermal insult, as detected by western blot and in-gel overlay analyses (Figure 1B). On the other hand, overexpression of Hsp70 (Ssa1) had no appreciable protective effect on the proteasome disassembly (data not shown).

Disassembly of the 26S proteasome caused by inactivation of Hsp90

In the next step, we examined the mechanism through which Hsp90 protects against disassembly of the 26S proteasome by severe thermal stress. For this purpose, we analyzed the structure of the 26S proteasome under defective conditions of Hsp90 using temperature-sensitive (ts^-) *hsp82–4Δhsc82* cells (YOK5) (hereafter, the mutant yeast is simply described as *hsp82-4* cells). First, we examined the 26S proteasome by the in-gel peptidase assay. As shown in Figure 2A (top), two slowly migrating active proteasomes, corresponding to R2C and RC, were evident in extracts of WT cells irrespective of the culture temperature (25 or 37°C). However, the signals corresponding to positions of R2C and RC markedly decreased when only samples prepared from *hsp82-4* cells that had been cultured for 8 h at non-permissive temperature of 37°C were used (Figure 2A). Activities similar to those of WT cell extracts were observed when extracts of *hsp82-4* cells cultured at permissive temperature were used. Moreover, the addition of SDS, which activates the latent 20S proteasome *in vitro*, caused marked activation of the 20S proteasome, and the magnitude of activation was augmented when we used the crude extracts of *hsp82-4* cells that had been cultured for 8 h at 37°C (Figure 2A, bottom). These results indicate that inactivation of Hsp90 causes dissociation of the active 26S proteasome into its constituents containing the 20S proteasome.

To confirm these observations, we loaded the samples prepared from WT and *hsp82-4* cells, which had been incubated for various times under a non-permissive temperature, onto native PAGE and SDS–PAGE, and then conducted western blotting with anti-20S proteasome. In the native PAGE, the three species of the proteasome, i.e. R2C, RC and C, were evident in WT cells even after 8 h incubation (Figure 2B, bottom). In contrast, destruction of both bands with lower electrophoretic mobility, corresponding to the R2C and RC forms of the 26S proteasome, began within only 4 h of inactivation of Hsp90, though it

took 8 h for their complete loss in *hsp82-4* cells. Consequently, loss of Hsp90 was associated with an increase in free 20S proteasome. However, the total amounts of the 20S proteasome analyzed by western blotting after SDS–PAGE, detected as several bands ranging from 20 to 35 kDa, remained unchanged. Thus it is clear that loss of function of Hsp90 causes dissociation of the 26S proteasome into its constituents, including the 20S proteasome. We then compared peptidase activities of the proteasome and cell viability under the same conditions. Both values were unchanged in WT cells, but the peptidase activities gradually decreased after around 4 h incubation at 37°C and almost completely disappeared upon incubation for 8 h in *hsp82-4* cells (Figure 2B, top). It was noteworthy that in these cells, the R2C form disappeared before the RC form and the activities of the proteasome were decreased (4 h after the shift), followed by the loss of the RC form (Figure 2B, top and bottom). Importantly, the loss of proteasome activities in *hsp82-4* cells occurred faster than cell death, indicating that the structural abnormality of the 26S proteasome is not due to cell death.

When the same electrophoretic and immunoblotting analyses were conducted using anti-Rpt1 (Figure 2C, left) and anti-Rpn12 (Figure 2D, left), the former is an ATPase base subunit and the latter is a non-ATPase lid subunit of RP (Glickman *et al.*, 1998), two slowly migrating R2C and RC bands were evident in native PAGE in all cases, except *hsp82-4* cells, under non-permissive temperature. Again, comparable amounts of Rpt1 and Rpn12 subunits of the RP complex were detected even under culture at 37°C by SDS–PAGE (see bottom panels). Intriguingly, excess loading of samples revealed the presence of Rpn12 and Rpn9, another lid subunit, at rapidly migrating positions, but their electrophoretic mobilities differed from each other (Figure 2E), indicating dissociation of the lid complex under defective Hsp90 conditions of the cells.

We also confirmed the involvement of Hsp90 in the maintenance of the 26S proteasome by shutting off Hsp82 expression using *GAL1* promoter. Repression of Hsp82 expression by replacement of galactose with glucose in the media resulted in the disappearance of the 26S proteasome (Figure 2C, right). Moreover, we observed that geldanamycin (GA), an Hsp90 inhibitor, caused loss of the 26S proteasome in *hsp82-4* cells even under permissive temperature, although it had no appreciable effects on the proteasomal states in WT cells (Figure 2D, right). These results strongly suggest that Hsp90 is essential for the 26S proteasome. Curiously, we repeatedly observed the sensitivity of *hsp82-4*, but not WT cells, to GA in both *in vivo* (Figures 2 and 3) and *in vitro* (Figure 4) analyses. The exact reason is unclear, but GA may be easily accessible to the active ATPase site of the *hsp82-4* protein, perhaps because of its abnormal conformation.

Hsp90-dependent in vivo assembly of the 26S proteasome

We first tested the physical interaction between Hsp90 and the 26S proteasome *in vivo*. For this purpose, we purified the 26S proteasome in a single step, using a Ni^+-resin column, from extracts of WT (J106) and *hsp82-4* cells (YOK5RH), whose *RPT1* was replaced by *6×His-RPT1*. The subunit composition of the enzyme from WT cells resembled that from *hsp82-4* cells grown at 25°C (data not shown). In both preparations, the addition of MG132 almost completely inhibited the hydrolysis activity of Suc-LLVY-AMC, revealing no contamination of other protease(s), and the specific activity of the purified 26S proteasome resulted in >10-fold increase in Suc-LLVY-AMC hydrolysis (data not shown). Intriguingly, compared with that WT cells, considerable amounts of Hsp82 were associated with affinity-purified 26S proteasome and larger amounts of Hsp90 were associated with the 26S proteasome from *hsp82-4* cells, as judged by the similar contents of various proteasomal subunits (Figure 3A, left), though the total Hsp90 contents in *hsp82-4* cell extracts were much less than those of the WT extracts because of the lack of Hsc82 in *hsp82-4* cells. Native PAGE and immunoblotting using anti-Hsp82 against Hsp82-depleted cells revealed that anti-Hsp82 reacted strongly with the R2C form than with RC form, but not appreciably with CP, indicating that Hsp82 associates with the 26S proteasome through the RP complex (Figure 3A, right). Intriguingly, even when the amounts of Hsp82 decreased to ~one-tenth of WT, Hsp82 only bound to R2C and RC (Figure 3A, right), indicating a high affinity of Hsp90 with the 26S proteasome.

We next examined the role of Hsp90 in the *in vivo* assembly of the 26S proteasome. When both WT and *hsp82-4* cells were grown at 25°C, the Suc-LLVY-AMC degrading activity of the 26S proteasome affinity-purified from the same amounts of crude cell extracts was almost similar, even when the peptidase assay was carried out at 37°C in the presence of ATP (time zero in Figure 3B, blue line). However, when *hsp82-4* cells were cultured for 8 h after a shift to 37°C, no appreciable amounts of proteasomal proteins were recovered by purifying operation using the same Ni^+-resin column, and consequently very little Suc-LLVY-AMC degrading activity was observed in the peptidase assay (data not shown). These results again indicated loss of the 26S proteasome under Hsp90-defective conditions of the cells.

In the next experiments, we examined whether, once disassembled, the proteasome in *hsp82-4* cells cultured under a non-permissive temperature could reassemble when the same Hsp90-inactivated cells were shifted to permissive temperature of 25°C. After heat shock at 37°C for 6 h, we added cycloheximide (CHX) to inhibit *de novo* protein synthesis (time zero in Figure 3B) and then these cells were shifted to 25°C for further culture. The 26S proteasome was affinity-purified from the same amount of cell extracts after reculture for the indicated time intervals. As shown in Figure 3B (right), 2 h after shifting to 25°C a considerable Suc-LLVY-AMC degrading activity was restored (black line). Of note, this restoration was independent of the newly synthesized proteasome because of the presence of CHX, suggesting the reassembly of the 26S proteasome subsequent to the functional recovery of Hsp90. Interestingly, this reactivation was diminished in GA-treated *hsp82-4* cells at the time of shift to 25°C and then was maintained at 25°C (red line), indicating that the ATPase function of Hsp90 is necessary for the restoration of the 26S proteasome. In contrast, continued culture in non-permissive temperature at 37°C was not associated with such increment in proteasomal peptidase activity (green line). In parallel analyses using WT cells

(Figure 3B, left), irrespective of heat shock, and *hsp82-4* cells under permissive temperature (Figure 3B, right, blue line), the Suc-LLVY-AMC degrading activities gradually diminished after addition of CHX. These results suggested that the restoration of peptidase activity is linked to the proper assembly of the 26S proteasome, assuming that the

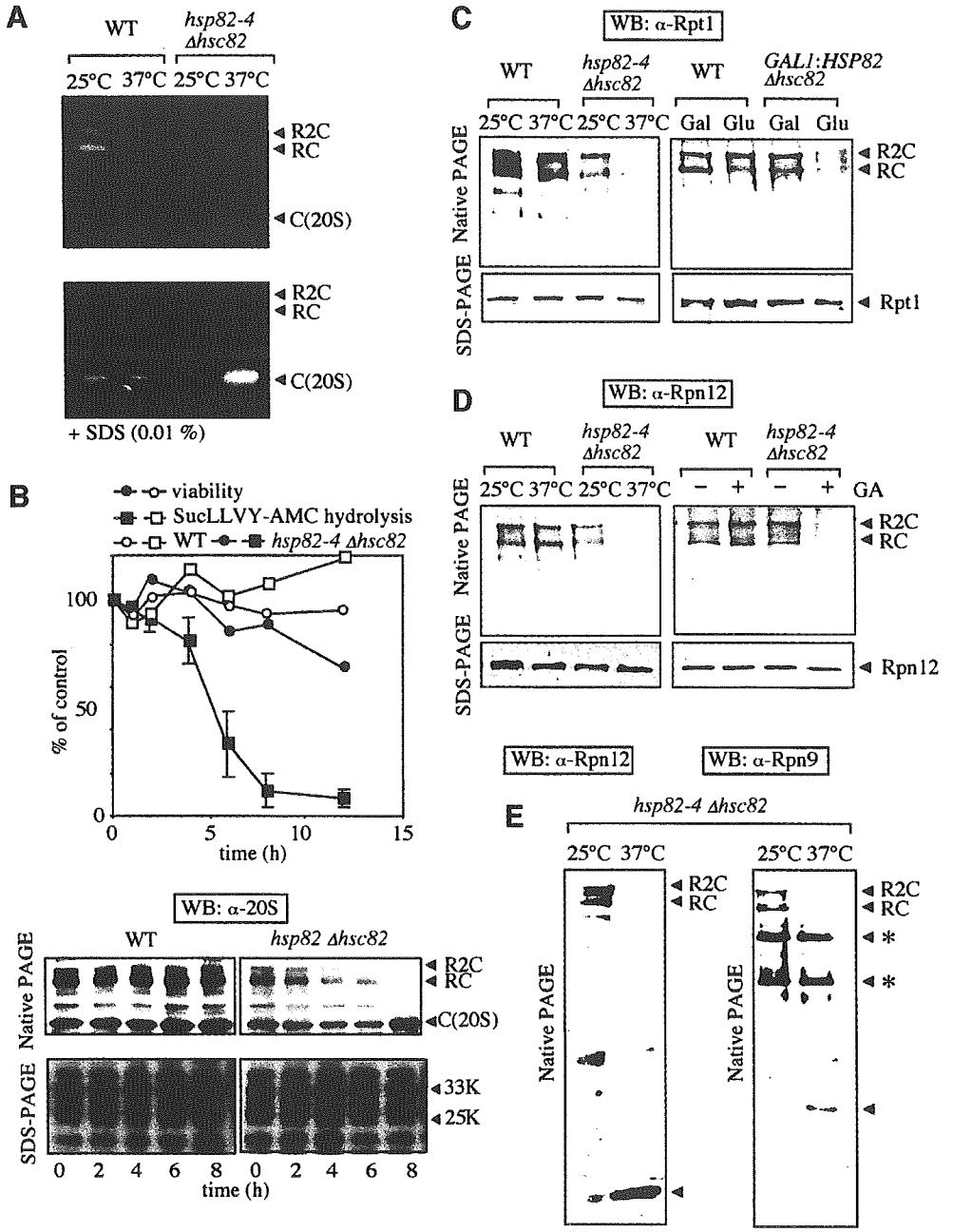

Fig. 2. Electrophoretic analyses of the 26S proteasome in *hsp82-4* cells. (**A**) In-gel overlay assay of peptidase activity of the proteasome separated by native PAGE. WT cells (YPH500) and *hsp82–4Δhsc82* cells (YOK5H) grown at 25°C were shifted at 37°C and maintained for another 8 h or continued culturing at 25°C. These cell extracts (20 μg) were analyzed as in Figure 1 in the presence of 2 mM ATP (top) or 0.01% SDS (bottom). (**B**) WT and *hsp82-4* cells grown at 25°C were shifted to 37°C and maintained for various times up to 12 h. Cells were sampled at each time point and then cell viability and Suc-LLVY-AMC degrading activity of the 26S proteasome affinity-purified were measured (top). The results are expressed relative to the result at time zero in WT cells. Open and closed squares represent activities of the 26S proteasome from WT and *hsp82-4* cells, respectively. Open and filled circles represent viability of WT and *hsp82-4* cells, respectively. Identical amounts of cell extracts were loaded onto native PAGE (top, 5 μg) and SDS–PAGE (bottom, 1 μg), followed by immunoblotting with anti-20S proteasome (bottom). (**C**) Western blotting with anti-Rpt1. The analyses were the same as for (B), except that anti-Rpt1 and 1 μg protein were used for native PAGE (left). The WT and *GAL1:HSP82 Δhsc82* cells (5CG2) grown at 30°C in YPGal were transferred to YPD and maintained for another 12 h or continued culturing in YPGal (right). The analyses were the same as for the left panel. (**D**) Western blotting with anti-Rpn12. The analyses were the same as for (B), except that anti-Rpn12 was used (left) and WT and *hsp82-4* cells grown at 25°C were treated (+) or mock treated (–) with GA (18 μM) followed by further culture at 25°C for 3 h (right). (**E**) Excess loading analyses. The same cell extracts in (D) for *hsp82-4* cells were analyzed by native PAGE and western blotting with anti-Rpn12 (left), except that 10 μg protein (lanes 1 and 2) was used. The same analysis was conducted using anti-Rpn9 and 10 μg protein (lanes 3 and 4). The band, indicated by arrowheads in both panels, was specific for antibodies against Rpn9 and Rpn12, respectively. Asterisks in the right panel indicate non-specific bands for anti-Rpn9.

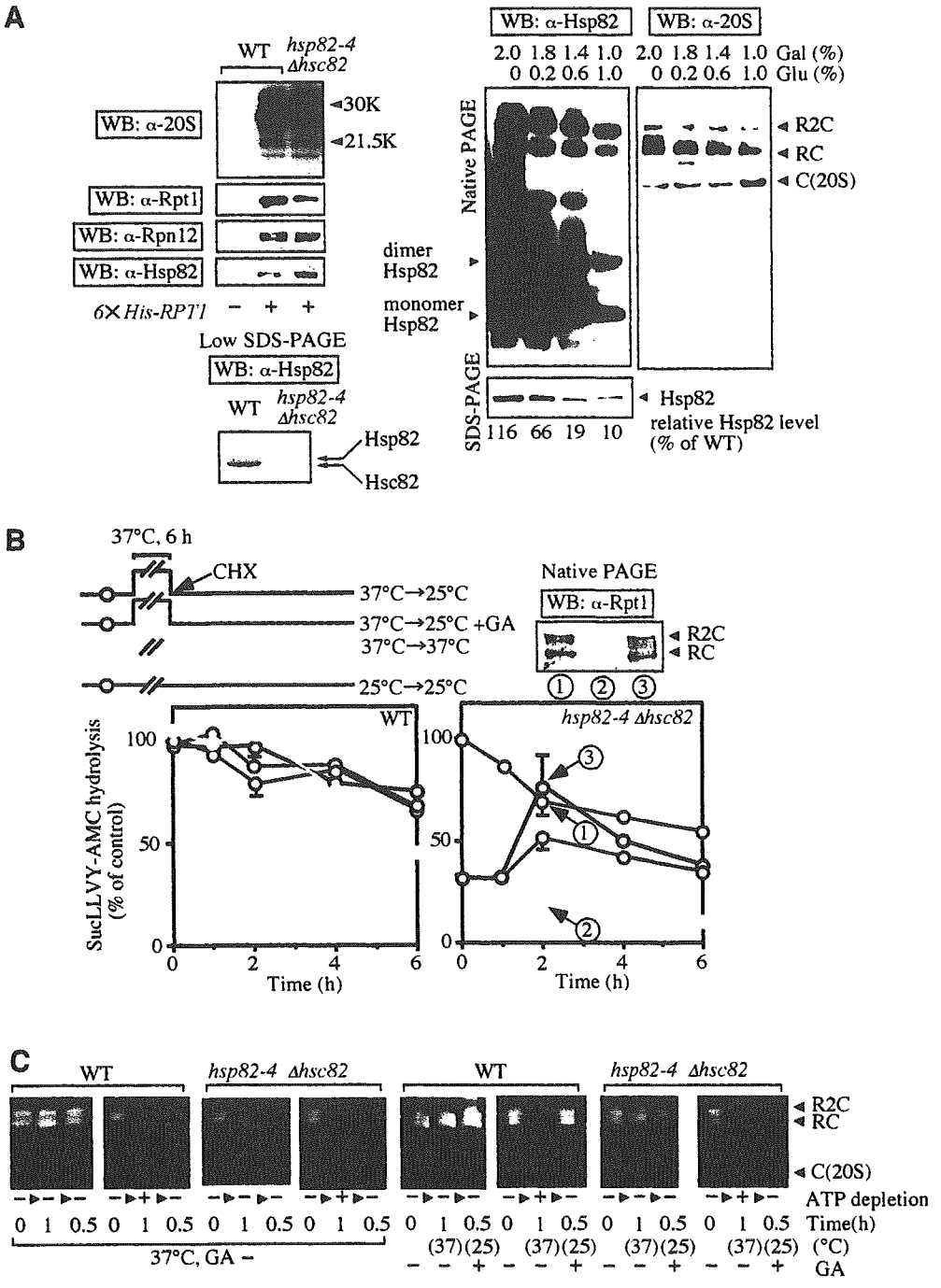

Fig. 3. *In vivo* analyses of the 26S proteasome under conditions with or without Hsp90 inactivation. (**A**) Western blotting was carried out with anti-Hsp82 and various proteasomal antibodies for the 26S proteasome (100 ng, left) affinity-purified from the extracts of WT (J106) and *hsp82–4Δhsc82* cells (YOK5RH) grown at 25°C by a Ni^{+}-resin column (–, YPH500, WT cells without *6×His-RPT1*). Western blotting after unconventional (low) SDS–PAGE (Imai and Yahara, 2000) was conducted to differentiate between Hsc82 and Hsp82 in the crude extracts (1 μg, left). Note that anti-Hsp82 reacted in a fashion similar to Hsc82 and Hsp82. Western blotting with anti-Hsp82 and anti-20S proteasome was carried out for Hsp82-depleted cells (5CG2) whose Hsp90 levels were varied by culturing with different combinations of Gal and Glu (right). The same amounts of cell extracts were loaded onto native PAGE (top, 5 μg) and SDS–PAGE (bottom, 1 μg), followed by immunoblotting with anti-Hsp82 and anti-20S proteasome. (**B**) WT (left) and *hsp82-4* cells (right) grown at 25°C were shifted to 37°C and maintained for an additional 6 h. At time zero, cells were shifted to the indicated temperatures followed by the addition of cycloheximide (CHX, 100 μg/ml). Cells were sampled at each time point and the Suc-LLVY-AMC degrading activity of the 26S proteasome affinity-purified as in (A) was measured. The activities are expressed relative to the activity at time zero in WT cells grown at 25°C. Blue lines, cells grown at 25°C throughout the experimental period; black lines, cells grown at 25°C were shifted to 37°C for 6 h and then to 25°C at time zero; red lines, similar to black lines except that the cells were treated with GA (18 μM) at time zero; green lines, cells grown at 25°C were shifted to 37°C for 6 h and further incubated at 37°C after time zero. Crude extracts (1 μg) of *hsp82-4* cells from positions denoted 1, 2 and 3 (right bottom) were separated by native PAGE and analyzed by western blotting with anti-Rpt1 (right top). Data are means ± SEM. (**C**) ATP requirement for Hsp90-dependent 26S proteasome assembly. WT and *hsp82-4* cells grown at 25°C were metabolically poisoned with 10 mM deoxyglucose and 10 mM sodium azide for 1 h at 37°C (designated + for ATP depletion). Cells cultured with YPD media without ATP-depletion are marked –. Thereafter, cells were shifted to YPD media for 30 min at 37°C (left panels) or YPD media containing GA (18 μM) for 30 min at 25°C (right panels). Activities of the 26S proteasome in gel-overlay assay were visualized as in Figure 1 with 2 mM ATP. Note that a considerable amount of Hsp90 is associated with the affinity-purified 26S proteasome fraction.

Hsp90 inactivation-induced disassembly of 26S proteasome is reversed by recovery of functional Hsp90. To confirm this attractive conclusion, we analyzed the 26S proteasome 2 h after incubation shown in Figure 3B (right, see arrows) by native PAGE and western blotting using anti-Rpt1. As shown in Figure 3B (right top), changes in activity apparently coincided with reassembly of both the R2C and RC forms of the 26S proteasome.

We next examined the ATP requirement for the Hsp90-dependent reassembly of the 26S proteasome. Depletion of ATP by treatment of cells with metabolic poisons (deoxyglucose and sodium azide) resulted in almost complete dissociation of the 26S proteasome, irrespective of WT and *hsp82-4* cells. When these cells were incubated for 30 min at 37°C in YPD media, reassembly of the 26S proteasome appeared in WT cells following culture in

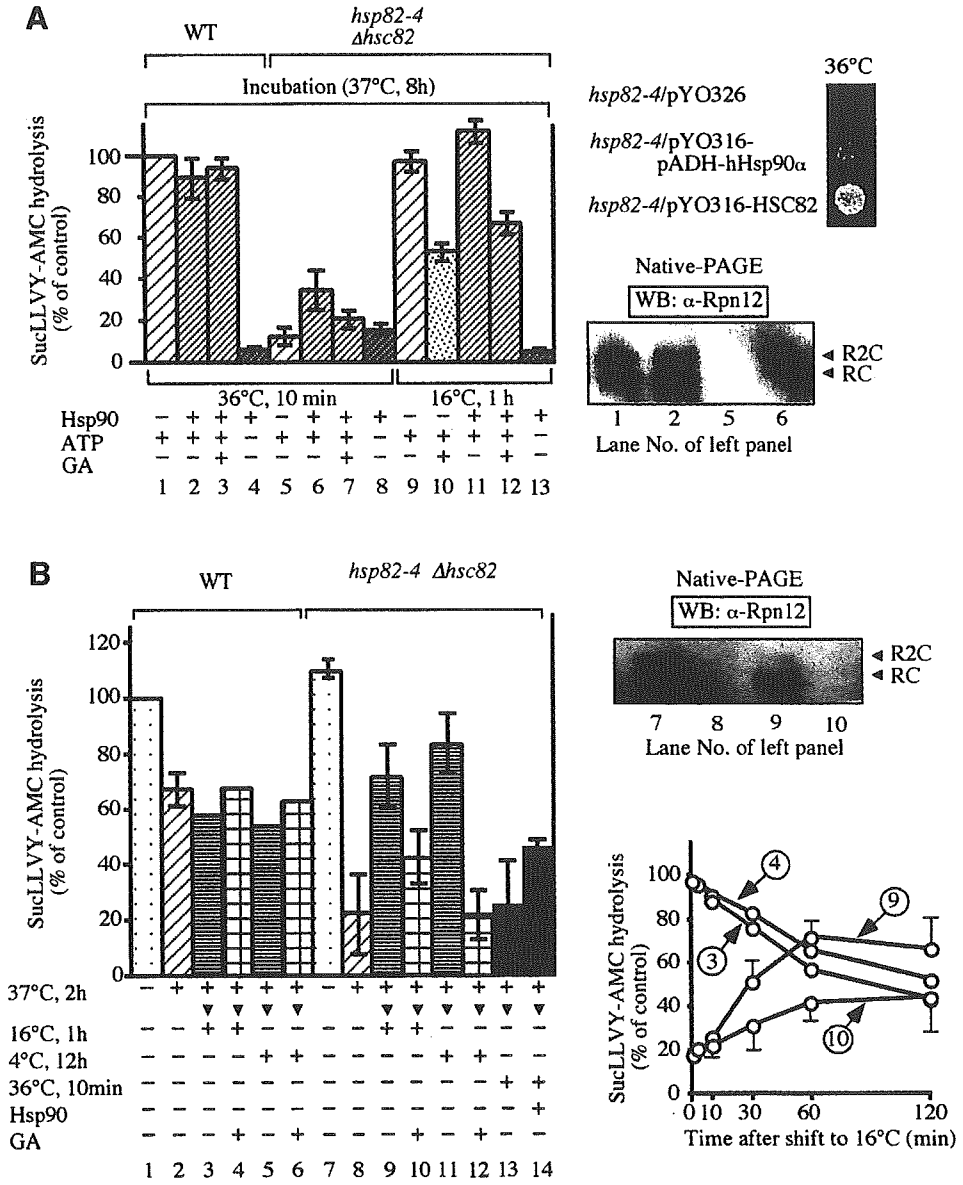

Fig. 4. *In vitro* analyses of the 26S proteasome under conditions with or without Hsp90 inactivation. (**A**) The Suc-LLVY-AMC degrading activities of the affinity-purified 26S proteasome from WT and *hsp82-4* cells were measured and expressed as percentages of the control (representing the activity of WT cell extracts without incubation). The extracts (10 mg/ml of protein) from both cells grown at 37°C for 8 h were incubated at 36°C for 15 min or at 16°C for 1 h with or without purified Hsp90 (0.1 mg/ml) and in the presence of an ATP-regeneration system (10 mM creatine phosphate, 5 mM $MgCl_2$ and 10 μg/ml of creatine kinase), an ATP-depletion system (10 mM glucose and 1 μg/ml of hexokinase) or GA (18 μM, left). The cell extracts corresponding to lanes 1, 2, 5 and 6 (left) were subjected to native-PAGE, followed by western blotting with anti-Rpn12 (right bottom). Each strain harboring the human-Hsp90α-expressing plasmid (YOK5H/pRS316-hHsp90α), the Hsc82-expressing plasmid (YOK5/pRS316-HSC82) or the vector alone (corresponding empty vector) was spotted on the same plates and incubated at 36°C for 2 days (right top). (**B**) *In vitro* inactivation and reactivation of the 26S proteasome from *hsp82-4* cells. The affinity-purified 26S proteasome from the same amounts of cell extracts of WT cells (J106) and *hsp82–4Δhsc82* cells (YOK5RH) were maintained at 37°C with an ATP-regenerating system for 2 h and shifted to 16°C for 1 h, 4°C for 12 h or 36°C for 10 min in the presence of an ATP-regenerating system with or without GA (18 μM) or purified Hsp90 (0.1 mg/ml)(left panel). Suc-LLVY-AMC hydrolysis is expressed relative to the activity at time zero of WT cells grown at 25°C. The affinity-purified 26S proteasomes corresponding to lanes 3, 4, 9 and 10 that had been treated at 37°C for 2 h were shifted to 16°C for various times as indicated, and thereafter Suc-LLVY-AMC hydrolysis was assayed as described above (right bottom panel). The affinity-purified 26S proteasomes corresponding to lanes 7–10 were subjected to native PAGE, followed by western blotting with anti-Rpn12 (right top panel). Data in A and B are means ± SEM.

glucose-containing (i.e. ATP-generating) YPD media, but not in *hsp82-4* cells, indicating the indispensable need for ATP in the Hsp90-dependent reassembly of the 26S proteasome (Figure 3C, left). Moreover, GA suppressed the assembly of the 26S proteasome in *hsp82-4* cells, but not WT extracts, at 25°C (Figure 3C, right). Taken together, the above results clearly showed that Hsp90 is required for the *in vivo* reassembly of the 26S proteasome even when this was partial, and, most importantly, the ATPase function of Hsp90 seems to play a pivotal role in this assembly process.

Hsp90-dependent in vitro reassembly of the 26S proteasome

In the next series of experiments, we examined whether Hsp90-dependent dissociation–reassociation of the 26S proteasome occurs in the *in vitro* system. Crude cell extracts were prepared from WT and *hsp82-4* cells grown at 37°C for 8 h, and subsequently incubated at 36°C for 10 min or 16°C for 1 h in the presence of an ATP-regenerating system, ATP-depleting system or GA, and, in some experiments, purified porcine Hsp90 was supplemented. Thereafter, Suc-LLVY-AMC degrading activity was assayed for the 26S proteasome affinity-purified from these cell extracts as shown in Figure 4A (left). The peptidase activity of the purified 26S proteasome decreased to nearly 10% from *hsp82-4* cells upon incubation for 8 h at 37°C compared with 26S proteasome from WT cell extracts, even when ATP was regenerated (see lane 5), but completely disappeared in the absence of ATP irrespective of temperature. Intriguingly, addition of purified Hsp90 caused partial suppression of the reduction in the presence of ATP (lane 6), indicating that Hsp90 is required for the *in vitro* assembly of functional 26S proteasome. Moreover, this Hsp90 effect was ATP dependent, because no obvious protective effect was detected under ATP-depletion conditions (lane 8). Addition of GA partially suppressed this reactivation (lanes 7, 10 and 12). It is noteworthy that *in vitro* reincubation of *hsp82-4* cell extracts for 1 h at 16°C caused almost complete recovery of the peptidase activity irrespective of Hsp90 supplementation (lanes 9 and 11). These findings suggest that Hsp90 promotes ATP-dependent reassembly of the 26S proteasome that had been dissociated by ts^--dependent Hsp90 inactivation.

We also confirmed that the activity change was proportional to the amounts of the purified 26S proteasome detected by western blotting with anti-Rpn12 (Figure 4A, bottom right). No appreciable amounts of the 26S proteasome were adsorbed by the Ni^+-resin column due to their disassembly in extracts of *hsp82-4* cells incubated *in vitro* at a restricted temperature. However, incubation of the same extracts supplemented with purified Hsp90 caused association of considerable amounts of the 26S proteasome with the affinity column, although the level of the recovered proteasome was somewhat low compared with similarly treated extracts of WT cells. These results indicate that Hsp90 is required for the *in vitro* reassembly of the 26S proteasome. Consistent with this notion, *in vivo* forced expression of Hsp90 rescued the growth defect of *hsp82-4* cells under non-permissive conditions, although yeast Hsc82 was effective compared with human Hsp90α (Figure 4A, right top).

To assess the above conclusion further, the 26S proteasome was inactivated and reactivated *in vitro* using the Ni^+-resin 26S proteasome purified from WT and *hsp82-4* cells grown at 25°C. Note that a considerable amount of Hsp90 is associated with the affinity-purified 26S proteasome fraction (see Figure 3A). Under incubation for 2 h at non-permissive temperature of 37°C, the purified 26S proteasome from *hsp82-4* cells showed rapid reduction of the peptidase activity, unlike WT enzymes, even after addition of an ATP-regeneration system (Figure 4B, left panel, lanes 2 and 8). This reduced activity of the 26S proteasome after 2 h of incubation at 37°C was markedly increased after incubation at 16°C for 1 h (lane 9) or at 4°C for 12 h (lane 11) in the presence of an ATP-regeneration system. However, no appreciable restoration of the peptidase activity was observed when an ATP-depletion system was added during incubation at 16°C or 4°C (data not shown), indicating again that metabolic energy is necessary for reactivation of the 26S proteasome. Addition of GA partially inhibited this reactivation (lanes 10 and 12), confirming the importance of ATPase function of Hsp90 for the reactivation, and presumably reassembly, of the 26S proteasome *in vitro*. In addition, such restoration was observed under *in vitro* incubation up to 60 min, which was clearly abrogated by addition of GA, although the activities of WT enzymes were gradually decreased, irrespective of GA (right bottom panel). In accordance with these results, when the 26S proteasome from *hsp82-4* cells that had been treated at 37°C for 2 h was incubated for 10 min at 36°C with purified Hsp90, the peptidase activity was partly recovered (Figure 4B, left panel, lanes 13 and 14). We also confirmed that the change in activity was proportional to the amount of the 26S proteasome detected by western blotting with anti-Rpn12 (Figure 4B, right top panel).

Genetic interactions between HSC82/HSP82 and genes encoding subunits of regulatory particle

To investigate the above findings *in vivo*, we examined genetic interactions using various proteasome mutants (Figure 5A). The *hsp82–4Δhsc82* double mutant showed severe growth defects when combined with mutants of *rpn1-1*, *Δrpn2* and *rpn3-1*. Although each parental strain showed no or only a weak growth defect at 30°C, the resultant triple mutants showed no growth at 30°C. When the combination of *rpn12-1* was examined, the effect was more severe because growth arrest occurred even when the cells were cultured at 25°C. Combination with *Δrpn10* was most surprising; the resultant triple mutant did not grow at all even at 25°C, although *Δrpn10* single mutation showed no growth defect even at 37°C (Figure 5B). On the other hand, overexpression of *HSC82* suppressed the ts^- growth defects of several mutants of the RP subunits of the 26S proteasome, such as *rpn1-1* cells, *Δrpn2* cells and *rpn3-1* cells (Figure 5C, top). Surprisingly, overexpression of Hsc82 inhibited the growth of *Δrpn10* cells and *rpn12-1* cells when they were cultured at 36°C and 25°C, respectively. At both temperatures, cells lacking the ectopically expressed Hsc82 showed no appreciable growth defect (Figure 5C, bottom). Thus genetic interactions between *HSC82/HSP82* and the genes encoding the RP subunits are strong, implying substantial interactions of the Hsp90 and the 26S proteasome.

In addition, even under permissive temperature of 25°C, GA caused severe growth defects in Δ*rpn10* and *rpn12-1* cells (Figure 5D, bottom), though its influence was less in *rpn1-1* and Δ*rpn2* cells (top). On the other hand, *Rpn3-1* cells showed obvious growth defect upon addition of GA at 30°C, but not at 25°C (Figure 5D, bottom). These findings support the genetic interactions between *HSC82/HSP82* and several proteasome genes.

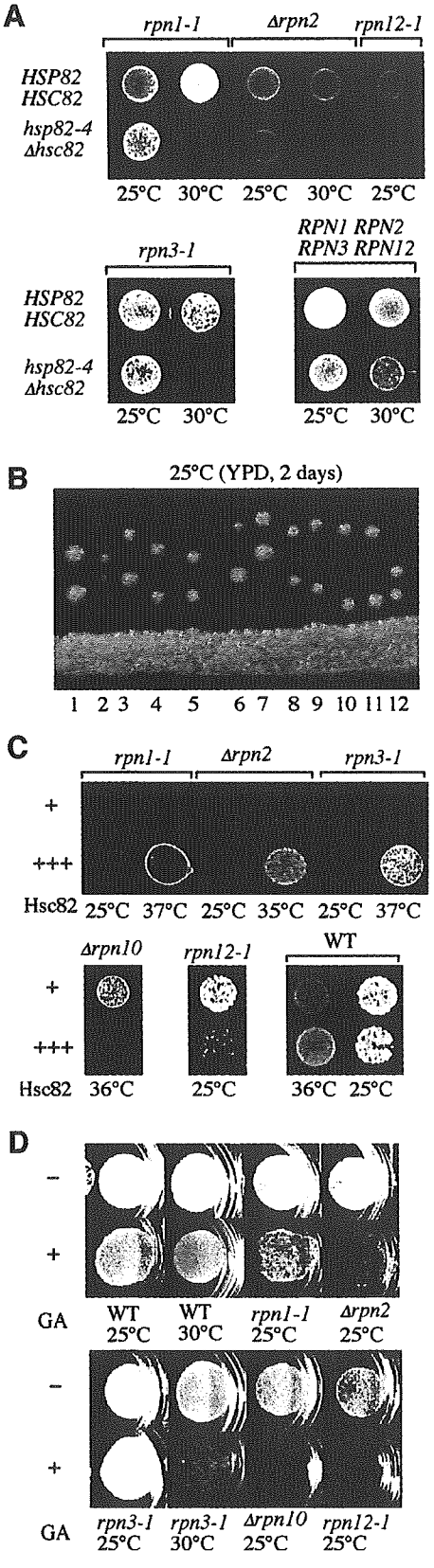

Effects of Hsc82 overexpression on 26S proteasome assembly in various proteasome mutants

Finally, we examined why overexpression of Hsp90 had opposing effects on cell proliferation, which was dependent on the type of mutation against the RP subunits of the 26S proteasome. Since our results showed that Hsp90 influenced the assembly of the 26S proteasome, we examined the role of Hsp90 on the 26S proteasome assembly. Since *HSC82* served as a multicopy suppressor of the temperature-sensitive growth of *rpn1-1* cells, Δ*rpn2* cells and *rpn3-1* cells (Figure 5C, top), we examined the molecular species of the proteasome in these cells using native PAGE followed by western blotting using anti-20S proteasome. Overexpression of Hsc82 suppressed the disassembly of the 26S proteasome in *rpn1-1* cells, Δ*rpn2* cells and *rpn3-1*cells under non-permissive temperatures of 37°C (*rpn1-1* cells and *rpn3-1* cells) and 34°C (Δ*rpn2* cells) (Figure 6A, middle and bottom panels), while absence of such overexpression markedly affected the disassembly of the 26S proteasome. In contrast, the inhibitory effects of overexpression of Hsc82 on Δ*rpn10* cells and *rpn12-1*cells (Figure 5C) appeared to be the results of disassembly of the 26S proteasome in these cells (Figure 6A, bottom). Note the appearance of several bands in these experiments, which were different from the main three bands observed initially which represented the 20S proteasome and the symmetric and asymmetric forms of the 26S proteasome. These extra bands represented incompletely assembled forms of the 26S proteasome, perhaps out by several components, because reactive bands by western blotting with anti-Rpt1 and anti-Rpn12 differed from each other and those with anti-20S proteasome (Figure 6A, middle). Furthermore, we confirmed peptidase activities of these extra bands by the in-gel peptidase assay (Figure 6B). Since the effects of overexpression of Hsc82 in various proteasome mutants correlate with the presence of the functional 26S proteasome, the above results also suggest that Hsp90 plays an important role in the regulation of assembly and disassembly of the 26S proteasome *in vivo*.

Fig. 5. Genetic interactions between HSC82/*HSP82* and various *RPN* genes. (**A**) Growth defects of triple mutants with *hsp82–4Δhsc82* together with *rpn1-1* (J821), Δ*rpn2* (J822), *rpn3-1* (J823) or *rpn12-1* (J8212). Each strain was spotted on YPD and incubated at the indicated temperatures for 2 days. (**B**) Synthetic lethality in Δ*rpn10* and *hsp82–4Δhsc82* mutations. JD8210 cells were sporulated and dissected. No germination of a Ura$^+$ His$^+$ Leu$^+$ colony corresponding to triple mutants was noted. Germination of small colonies was noted, though rarely (e.g. lanes 3 and 8). (**C**) Effects of overexpression of Hsc82. Each strain harboring HSC82 (+++) overexpressing plasmid (YPH500/pYO326-HSC82, JR1/pYO323-HSC82, JR2/pYO323-HSC82, JR3/pYO325-HSC82, JR10/pYO326-HSC82, JR12/pYO326-HSC82) and the vector alone (corresponding empty vector) (+) was spotted on SD plates containing appropriate amino acids and incubated at the indicated temperatures for 2 days. Note that the expressed levels of Hsc82 were not affected by these proteasomal mutations (data not shown). (**D**) Sensitivity to GA in various *rpn* mutants. Each strain used in A was spotted with or without GA (18 μM) and incubated for 2 days at indicated temperatures.

Discussion

The 26S proteasome is an unusually large complex, consisting of two subcomplexes, CP and RP. A major challenge to our understanding of the quaternary structure is how the large complex, composed of many subunits of various sizes, is accurately assembled in the cells. Recent studies of 20S proteasome assembly have shown that a key molecule termed 'Ump1' functions as a core factor to gather multiple proteasomal β-subunits (Ramos *et al.*, 1998). At present, however, little is known about the mechanism(s) involved in the assembly of the 26S proteasome, especially the RP complex.

In the present study, we showed that inactivation of Hsp90, using yeast mutants, caused almost complete disassembly of the 26S proteasome, indicating that Hsp90 plays a role in keeping the structural integrity of this large complex (Figure 2). Inactivation of Hsp90 resulted in dissociation of the 26S proteasome into the core 20S particle, which settled into a latent state, as evidenced by the marked activation upon the addition of SDS (Figure 2A). In contrast, Rpn9 and Rpn12 subunits migrated to different positions in native PAGE (Figure 2E), indicating loss of integrity of the lid complex. However, it is not known whether these lid subunits dissociated into their monomeric forms. It is also not known how Hsp90 influences the organization of the base complex, but it is clear at least that the functional loss of Hsp90 triggers disruption of the RP complex. These findings indicate that the RP complex is structurally fragile, requiring continuous supply of a functional Hsp90 to assemble and maintain these complexes, unlike the 20S proteasome, which is apparently stable without functional Hsp90. Thus the assemblies of the CP/20S proteasome and RP complexes are mechanistically different.

The genetic evidence provided in the present study also strongly suggests *in vivo* linkage between Hsp90 and the 26S proteasome. In fact, we demonstrated that overexpression of Hsc82 suppressed ts⁻ growth defects of *rpn1-1* cells, Δ*rpn2* cells and *rpn3-1* cells (Figure 5C) and prevented dissociation of the 26S proteasome, which occurred under conditions otherwise non-permissive for these mutants (Figure 6). Consistent with this genetic interaction, *hsp82–4Δhsc82* showed weak synthetic lethality with those proteasomal mutations (Figure 5A). Furthermore, strong synthetic lethality was observed between *hsp82–4Δhsc82* and Δ*rpn10* or *rpn12-1*. Interestingly, even though the Δ*rpn10* mutation itself showed no growth defect at all, it exhibited the most severe growth defect when combined with *hsp82–4Δhsc82* mutant (Figure 5B and D). However, overexpression of Hsc82 in Δ*rpn10* cells and *rpn12-1* cells enhanced their growth defects and was associated with decreased 26S proteasome levels in these two strains (Figure 6). One possible explanation for these antagonizing effects is that the tight interaction between Hsp90 and some subunits of regulatory particle might hinder them from proper formation of the 26S proteasome, leading to inhibition of cellular proliferation.

We obtained evidence that a larger amount of Hsp90 is associated with the 26S proteasome from *hsp82-4* cells grown at permissive temperature, compared with the WT proteasome, irrespective of the lower content of Hsp90 in mutant cell extracts (Figure 3A, left), suggesting that the larger amount of mutant Hsp90 might be required to maintain the 26S proteasome because of its functional impairment. We also found that considerable amounts of Hsp90 are associated with the 26S proteasome through the RP complex, and this association is so tight that it occurs even under low Hsp90 conditions in which many other client proteins were dissociated from Hsp90 (Figure 3A, right). In addition, *hsp82-4* cells showed a faster decay of

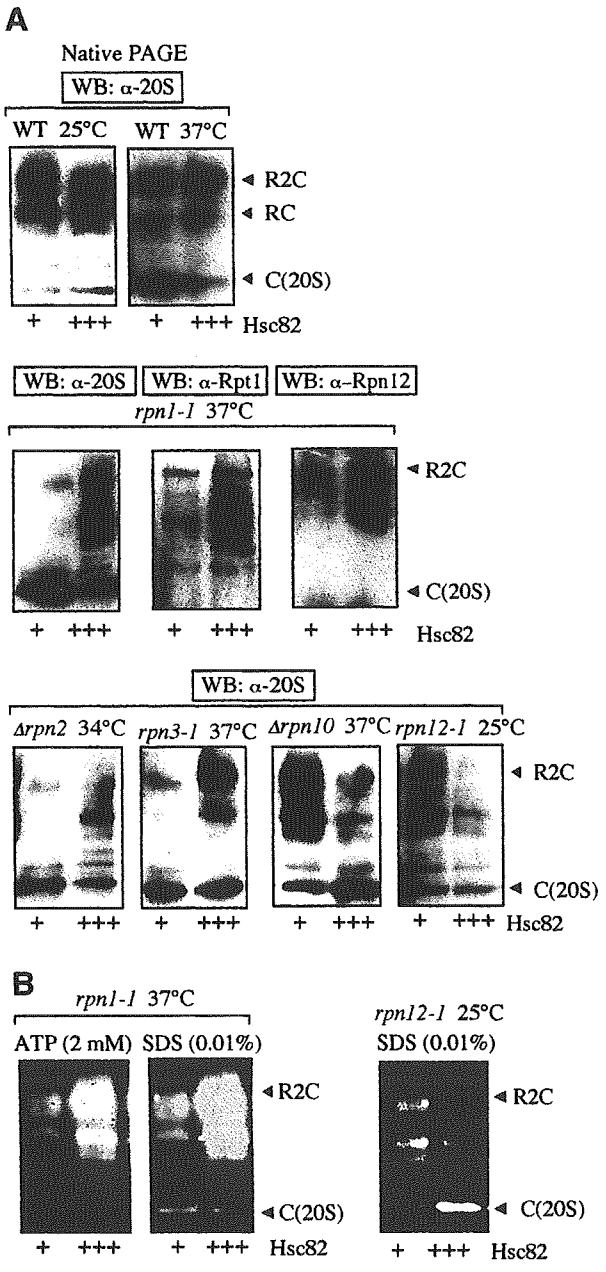

Fig. 6. Effects of overexpression of Hsc82 on the 26S proteasome assembly in various *rpn* mutants. (**A**) WT cells and various proteasome mutant cells harboring control plasmid (+), multicopy plasmid carrying *HSC82* (+++), as in Figure 5C, grown at 25°C were shifted to the indicated temperatures and incubated for an additional 8 h. Samples of cell lysates (5 μg) were loaded onto native PAGE and analyzed by western blotting with anti-20S proteasome, anti-Rpt1 or anti-Rpn12. (**B**) Corresponding cell extracts as in (A) were analyzed by gel-overlay assay as in Figure 1 with 2 mM ATP or 0.01% SDS.

Table I. Yeast strains used in this study

Strain	Source	Genotype
YPH500	*MATα ura3 lys2 ade2 trp1 his3 leu2*	Sikorski and Hieter, 1989
YOK5	*MAT***a** *ura3 lys2 ade2 trp1 his3 leu2 Δhsc82::URA3 hsp82-4::LEU2*	Kimura *et al.*, 1994
YOK5H	*MAT***a** *ura3 lys2 ade2 trp1 his3 leu2 Δhsc82::HIS3 hsp82-4::LEU2*	Our laboratory stock
YOK5RH	*MAT***a** *ura3 lys2 ade2 trp1 his3 leu2 Δhsc82::HIS3 hsp82-4::LEU2 6×His-RPT1::URA3*	Present study
5CG2	*MAT***a** *ura3 lys2 ade2 trp1 his3 leu2 Δhsc82::URA3 hsp82-4::GAL1-HSP82::LEU2*	Kimura *et al.*, 1994
J106	*MATα 6×His-RPT1::URA3 ura3 lys2 ade2 trp1 his3 leu2*	Takeuchi *et al.*, 1999
YK109	*MAT***a** *ura3 lys2 ade2 trp1 his3 leu2 rpn12-1*	Kominami *et al.*, 1997
JR1	*MAT***a** *ura3 lys2 ade2 trp1 his3 leu2 rpn1-1*	Present study
J821	*MAT***a** *ura3 lys2 ade2 trp1 his3 leu2 Δhsc82::HIS3 hsp82-4::LEU2 rpn1-1*	Present study
JR2	*MAT***a** *ura3 lys2 ade2 trp1 his3 leu2 Δrpn2::URA3*	Present study
J822	*MAT***a** *ura3 lys2 ade2 trp1 his3 leu2 Δhsc82::HIS3 hsp82-4::LEU2 Δrpn2::URA3*	Present study
JR3	*MAT***a** *ura3 lys2 ade2 trp1 his3 leu2 rpn3-1::HIS3*	Present study
J823	*MAT***a** *ura3 lys2 ade2 trp1 his3 leu2 Δhsc82::URA3 hsp82-4::LEU2 rpn3-1::HIS3*	Present study
JR10	*MAT***a** *ura3 lys2 ade2 trp1 his3 leu2 Δrpn10::HIS3*	Present study
JR12	*MAT***a** *ura3 lys2 ade2 trp1 his3 leu2 rpn12-1*	Present study
J8212	*MAT***a** *ura3 lys2 ade2 trp1 his3 leu2 Δhsc82::HIS3 hsp82-4::LEU2 rpn12-1*	Present study
J38	*MATα leu2 his3 ura3 trp1 Δrpn10::HIS3*	Takeuchi *et al.*, 1999
JD8210	*MAT***a**/α *ura3/ura3 lys2/lys2 ade2/ade2 trp1/trp1 his3/his3 leu2/leu2 Δhsc82::URA3/Δhsc82::URA3 hsp82-4::LEU2/hsp82-4::LEU2 RPN10/Δrpn10::HIS3*	Present study
rpn1::URA3	*MATα ura3 lys2 ade2 trp1 his3 leu2 rpn1::URA3 (rpn1-1)*	Our laboratory stock
W1646–1C	*MATα leu2 his3 ura3 trp1 ade2 Δrpn2::URA3*	Our laboratory stock
YK137	*MAT***a** *leu2 his3 ura3 trp1 rpn3-1::HIS3*	Kominami *et al.*, 1997

the peptidase activities of the 26S proteasome after addition of CHX even under permissive temperature compared with WT cells (Figure 3B). Taken together, these results suggest that the 26S proteasome is the most important substrate for Hsp90, and Hsp90 is continually required for maintenance of the 26S proteasome.

The energy requirement for 26S proteasome assembly has been recognized since the discovery of the 26S proteasome (Armon *et al.*, 1990; Driscoll and Goldberg, 1990; Chu-Ping *et al.*, 1994), but the molecular mechanisms of ATP consumption have remained elusive. In the present study, we have provided evidence that ATPase of Hsp90 plays an active role in supplying energy required for the 26S proteasome assembly. Thus, we have shown that the dissociated constituents of the 26S proteasome from *hsp82-4* cells under non-permissive conditions, reassembled *in vivo* and *in vitro* by reactivation of ts$^-$ Hsp82 or addition of purified Hsp90 (Figures 3 and 4). Although the reason for not being able to get the full restoration by purified Hsp90 *in vitro* is not clear at present, it is plausible that Hsp90 acts in concert with various cochaperones, such as p23 (Young *et al.*, 2001), to exert its full activity, some of which might be lost in the purification of Hsp90 by the present technique. More importantly, we demonstrated that ATP is required for Hsp90-dependent reassembly and that inhibition of Hsp90-ATPase function by GA also blocked in part this restoration of the 26S proteasome. Thus we propose that the energy required for the assembly of the 26S proteasome is at least utilized by Hsp90.

An important question is whether the dissociation–association cycle of the 26S proteasome has any physiological significance. An intriguing scenario is that a dissociation–association cycle might be envisaged for the 26S proteasome or it might be regulated to respond to changes in certain environmental circumstances in cells. For example, marked increases have been found in the amounts of the 26S proteasome during the stationary phase compared with those in logarithmically growing yeast cells (Fujimuro *et al.*, 1998). In this regard, it is interesting to note that yeast Hsp90 also increases during the stationary phase (Iida and Yahara, 1984), implying that Hsp90 may contribute to these dynamic alterations, repeating assembly and disassembly in logarithmic/stationary phase shift. In addition, the involvement of an Hsp90 chaperone in the assembly of the 26S proteasome indicates that changes in the physiological state of Hsp90 may alter the amounts of the 26S proteasome. In fact, we initially found that the amounts of the 26S proteasome decreased upon exposure to the thermal insult of 50°C but showed full recovery within 6–8 h after the temperature was reversed to 25°C (Figure 1). In this regard, previous studies reported that the cellular ATP level remained largely unchanged under such severe heat shock conditions (Jamsa *et al.*, 1995), indicating that disassembly of the 26S proteasome is not due to reduced availability of ATP. However, such temporary reductions in the 26S proteasome are conceivable because while Hsp90 is required for the 26S proteasome assembly, it is also responsible for refolding stress-damaged proteins and thereby might be sequestered to those damaged proteins after severe thermal insults. Thus it is conceivable to view the disassembly of the 26S proteasome as a stress response regulated by Hsp90. In other words, our results highlight the importance of Hsp90 in the disassembly–reassembly cycle of the 26S proteasome, although further studies are necessary to determine its precise molecular action.

Materials and methods

Microbiological techniques

Experimental methods for yeast were performed as described (Guthrie and Fink, 1991). Yeast cells were cultured in YPD on logarithmically growing phase, unless otherwise indicated.

Plasmids

Plasmids pYO323-HSC82 and pYO325-HSC82 carry the 4.2 kbp *Spe*I–*Spe*I fragments of *HSC82* in the *Xba*I site of pYO323 and pYO325 (Ohya *et al.*, 1991), respectively. Plasmids pYO326-HSC82 (Imai and Yahara, 2000) and pRS316-pADH-hHsp90α were our laboratory stock.

Antibodies and reagents

Rabbit polyclonal anti-Rpn9 and anti-Rpn12 antibodies were a kind gift from Dr A.Toh-e (Tokyo University). Rabbit polyclonal anti-Rpt1 (Takeuchi *et al.*, 1999), anti-20S proteasome (Tanaka *et al.*, 1988) and anti-Hsp82 (Imai and Yahara, 2000) antibodies were used. Purified porcine Hsp90 was our laboratory stock. Suc-LLVY-AMC was obtained from Peptide Institute Inc. CHX, deoxyglucose and azide were purchased from Sigma Chemical Co. (St Louis, MO). GA was obtained from Gibco BRL (Gaithersburg, MD). Protein concentration was determined using BCA protein assay reagent (Pierce Chemical Co.) with bovine serum albumin (Sigma) as the standard.

Strains

The yeast strains used are listed in Table I. Strains referred to in this study were constructed by conventional genetic methods.

Electrophoresis

We used 10–20% and 7.5–15% (Figure 2B only) gradient gel for SDS–PAGE and 2–15% polyacrylamide gradient gel (Daiichi Pure Chemical Co.) for native PAGE.

Western blotting

The crude cell extracts were subjected to SDS–PAGE or native PAGE, transferred onto a PVDF membrane. Then the blot was developed with the indicated primary antibodies, horseradish peroxidase conjugated secondary antibodies and the chemiluminescent substrate.

Peptidase activity

Peptidase activity was assayed using Suc-LLVY-AMC as a substrate. Suc-LLVY-AMC (0.1 mM) was incubated with an enzyme source for 10 min at 37°C as described previously (Tanaka *et al.*, 1988). The activities are expressed as averages of three independent experiments or as mean ± SEM. The overlay assay of peptidase activities of the proteasome after native PAGE was described previously (Glickman *et al.*, 1998). Peptidase activity was visualized by irradiating the gel with 380 nm UV light.

Preparation of crude extracts

Yeast cells were harvested and washed once with ice-cold lysis buffer (100 mM Tris–HCl pH 7.6, 2 mM ATP, 0.5 mM EDTA, 2 mM $MgCl_2$ and 2% glycerol), and then disrupted with glass beads in 200 µl of lysis buffer. After removal of unbroken cells and glass beads by brief centrifugation at 100 *g*, the extracts were clarified by centrifugation twice at 20 000*g* and 4°C for 10 min. The final supernatant was used as the crude extract.

Affinity-purification of 26S proteasome

Purification of 26S proteasome by Ni-nitrilotriacetic acid (NTA) affinity chromatography was performed. Briefly, the yeast extracts were clarified by centrifugation at 100 000 *g* at 4°C for 30 min. The supernatant was subjected to ultracentrifugation at 235 000 *g* and 4°C for 5 h to precipitate the proteasome. The resulting precipitates were gently dissolved in 10 ml of buffer A (20 mM Tris–HCl pH 7.8, 1 mM ATP, 0.1 mM EDTA, 2 mM $MgCl_2$, 100 mM NaCl and 10% glycerol) with an ATP regeneration system. After removal of insoluble materials by centrifugation at 9100 *g* and 4°C for 10 min, the resulting supernatant was loaded onto a Ni^+-NTA–agarose column (Qiagen, Hilden, Germany). After washing the column with buffer A containing 50 mM imidazole, the His-tagged column associated with the proteasome was eluted with elution buffer (buffer A with 200 mM imidazole). In successive experiments, the 26S proteasome was purified from the same volume of cell extracts containing the same amount of protein.

References

Armon,T., Ganoth,D. and Hershko,A. (1990) Assembly of the 26S complex that degrades proteins ligated to ubiquitin is accompanied by the formation of ATPase activity. *J. Biol. Chem.*, **265**, 20723–20726.

Baumeister,W., Walz,J., Zuhl,F. and Seemuller,E. (1998) The proteasome: paradigm of a self-compartmentalizing protease. *Cell*, **92**, 367–380.

Chu-Ping, M., Vu,J. H, Proske,R.J., Slaughter,C.A. and DeMartino,G.N. (1994) Identification, purification and characterization of a high molecular weight, ATP-dependent activator (PA700) of the 20S proteasome. *J. Biol. Chem.*, **269**, 3539–3547.

Driscoll,J. and Goldberg,A.L. (1990) The proteasome (multicatalytic protease) is a component of the 1500-kDa proteolytic complex which degrades ubiquitin-conjugated proteins. *J. Biol. Chem.*, **265**, 4789–4792.

Frydman,J. (2001) Folding of newly translated proteins *in vivo*: the role of molecular chaperones. *Annu. Rev. Biochem.*, **70**, 603–647.

Fujimuro,M., Takada,H., Saeki,Y., Toh-e,A., Tanaka,K. and Yokosawa,H. (1998) Growth-dependent regulation of the 26S proteasome assembly in the budding yeast *Saccharomyces cerevisiae*. *Biochem. Biophys. Res. Commun.*, **251**, 818–823.

Glickman,M.H., Rubin,D.M., Coux,O., Wefes,I., Pfeifer,G., Cjeka,Z., Baumeister,W., Fried,V.A. and Finley,D. (1998) A subcomplex of the proteasome regulatory particle required for ubiquitin-conjugate degradation and related to the COP9 signalosome and eIF3. *Cell*, **94**, 615–623.

Guthrie,C. and Fink,G.R. (eds) (1991) Guide to yeast genetics and molecular biology. Academic Press, San Diego, CA.

Iida,H. and Yahara,I. (1984) Durable synthesis of high molecular weight heat shock proteins in G_0 cells of the yeast and other eucaryotes. *J. Cell Biol.*, **99**, 199–207.

Imai,J. and Yahara,I. (2000) Role of HSP90 in salt stress tolerance via stabilization and regulation of calcineurin. *Mol. Cell. Biol.*, **20**, 9262–9270.

Jamsa,E., Vakula,N., Arffman,A., Kilpelainen,I. and Makarow,M. (1995) *In vivo* reactivation of heat-denatured protein in the endoplasmic reticulum of yeast. *EMBO J.*, **14**, 6028–6033.

Kimura,Y., Matsumoto,S. and Yahara,I. (1994) Temperature-sensitive mutants of hsp82 of the budding yeast *Saccharomyces cerevisiae*. *Mol. Gen. Genet.*, **242**, 517–527

Kominami,K. *et al.* (1997) Yeast counterparts of subunits S5a and p58 (S3) of the human 26S proteasome are encoded by two multicopy suppressors of nin1-1. *Mol. Biol. Cell*, **8**, 171–187.

Ohya,Y., Umemoto,N., Tanida,I., Ohta,A., Iida,H. and Anraku,Y. (1991) Calcium-sensitive cls mutants of *Saccharomyces cerevisiae* showing a Pet^- phenotype are ascribable to defects of vacuolar membrane H(+)-ATPase activity. *J. Biol. Chem.*, **266**, 13971–13977.

Panaretou B., Prodromou C., Roe S.M., O'Brien R., Ladbury J.E., Piper P.W. and Pearl L.H. (1998) ATP binding and hydrolysis are essential to the function of the Hsp90 molecular chaperone *in vivo*. *EMBO J.*, **17**, 4829–4836.

Pickart,C.M. (2001) Mechanisms underlying ubiquitination. *Annu. Rev. Biochem.*, **70**, 503–533.

Ramos,P. C, Hockendorff,J., Johnson,E.S., Varshavsky,A. and Dohmen,R.J. (1998) Ump1p is required for proper maturation of the 20S proteasome and becomes its substrate upon completion of the assembly. *Cell*, **92**, 489–499.

Richter,K. and Buchner,J. (2001) Hsp90: chaperoning signal transduction. *J. Cell. Physiol.*, **188**, 281–290.

Sherman,M.Y. and Goldberg,A.L. (2001) Cellular defences against unfolded proteins: a cell biologist thinks about neurodegenerative diseases. *Neuron*, **29**, 15–32.

Sikorski,R.S. and Hieter,P. (1989) A system of shuttle vectors and yeast host strain designed for efficient manipulation of DNA in *Saccharomyces cerevisiae*. *Genetics*, **122**, 19–27.

Takeuchi,J., Fujimuro,M., Yokosawa,H., Tanaka,K. and Toh-e,A. (1999) Rpn9 is required for efficient assembly of the yeast 26S proteasome. *Mol. Cell. Biol.*, **19**, 6575–6584.

Tanaka,K., Yoshimura,T., Kumatori,A., Ichihara,A., Ikai,A., Nishigai,M., Kameyama,K. and Takagi,T. (1988) Proteasomes (multi-protease complexes) as 20S ring-shaped particles in a variety of eukaryotic cells. *J. Biol. Chem.*, **263**, 16209–16217.

Young,J.C., Moarefi,I. and Hartl,F.U. (2001) Hsp90: a specialized but essential protein-folding tool. *J. Cell Biol.*, **154**, 267–273.

Received January 20, 2003; revised May 20, 2003; accepted May 21, 2003

THE JOURNAL OF BIOLOGICAL CHEMISTRY
Vol. 278, No. 44, Issue of October 31, pp. 43877–43884, 2003
Printed in U.S.A.

Fbs2 Is a New Member of the E3 Ubiquitin Ligase Family That Recognizes Sugar Chains*

Received for publication, April 21, 2003, and in revised form, August 22, 2003
Published, JBC Papers in Press, August 25, 2003, DOI 10.1074/jbc.M304157200

Yukiko Yoshida‡§¶, Fuminori Tokunaga§‖, Tomoki Chiba‡, Kazuhiro Iwai§‖, Keiji Tanaka‡, and Tadashi Tai‡§

From the ‡Tokyo Metropolitan Institute of Medical Science, Bunkyo-ku, Tokyo 113-8613, Japan, the §Core Research for Engineering, Science, and Technology (CREST), Japan Science and Technology Corporation (JST), Saitama 332-0012, Japan, and the ‖Department of Molecular Cell Biology, Graduate School of Medicine, Osaka City University, Osaka 545-8585, Japan

F-box proteins are substrate recognition components of Skp1-Cullin1-F-box protein-Roc1 (SCF) E3 ubiquitin-protein ligases. We reported previously that Fbs1 (F-box protein that recognizes sugar chains; equivalent to Fbx2 or NFB42) binds specifically to proteins attached with high mannose oligosaccharides and subsequently contributes to elimination of *N*-glycoproteins in cytosol (Yoshida, Y., Chiba, T., Tokunaga, F., Kawasaki, H., Iwai, K., Suzuki, T., Ito, Y., Matsuoka, K., Yoshida, M., Tanaka, K., and Tai, T. (2002) *Nature* 418, 438–442). Here we report the identification of another F-box protein that recognizes *N*-glycan, Fbs2 (called Fbx6b or FBG2 previously). Although the expression of Fbs1 was restricted to the adult brain and testis, the Fbs2 transcript was widely expressed. The Fbs2 protein forms an SCF^{Fbs2} ubiquitin-ligase complex that targets sugar chains in *N*-glycoproteins for ubiquitylation. Only glycoproteins bound to concanavalin A lectin and not to wheat germ agglutinin or *Ricinus communis* agglutinin interacted with Fbs2 in various tissues and cell lines. Pull-down analysis using various oligosaccharides revealed that $Man_{3-9}GlcNAc_2$ glycans were required for efficient Fbs2 binding, whereas modifications of mannose residues by other sugars or deletion of inner GlcNAc reduced Fbs2 binding. Fbs2 interacted with *N*-glycans of T-cell receptor α-subunit (TCRα), a typical substrate of the endoplasmic reticulum-associated degradation (ERAD) pathway, and the forced expression of mutant Fbs2ΔF, which lacks the F-box domain essential for forming the SCF complex, and decrease of endogenous Fbs2 by small interfering RNA led to inhibition of TCRα degradation in cells. Thus, Fbs2 is a novel member of F-box protein family that recognizes *N*-glycans and plays a role in ERAD.

Selective protein degradation by the ubiquitin-proteasome pathway serves as a powerful regulatory mechanism in a wide variety of cellular processes. Ubiquitin conjugation requires the sequential activities of three enzymes or protein complexes called the ubiquitin-activating enzyme (E1),[1] the ubiquitin-conjugating enzyme (E2), and the ubiquitin-protein ligase (E3) (1). In the ubiquitin pathway, E3 plays an important role in the selection of target proteins for degradation, because each distinct E3 usually binds a protein substrate with a degree of selectivity for ubiquitylation. E3s are believed to exist as molecules with a large diversity, presumably in more than hundreds of species, which are classified into many subfamilies. One of the best characterized E3 families is the Skp1-Cullin1-F-box protein-Roc1 (SCF) complex (2). The SCF is composed of a Cullin1/Cdc53, Skp1, Roc1/Rbx1/Hrt1, and one member of a large family of proteins called F-box proteins. F-box proteins typically have a bipartite structure with an N-terminal F box motif consisting of ~40 amino acid residues and a C-terminal region that interacts with the substrate and, thereby, the function of the F-box protein is to trap target proteins (3, 4). However, it remains elusive how E3s accurately recognize target proteins. Accumulating evidence suggests that phosphorylation of target proteins is a prerequisite for their recognition by SCF complexes (1, 2, 4). In addition, it has been shown that proline hydroxylation of the transcription factor hypoxia-induced factor 1α (HIF1α) serves as a signal for ubiquitylation by the SCF-like Cullin2-based VBC ubiquitin-ligase (5, 6). On the other hand, we have reported recently that Fbx2 forms an SCF^{Fbx2} ubiquitin ligase complex that targets sugar chains in *N*-linked glycoproteins for ubiquitylation (7). Thus, Fbx2 is a novel example of F-box proteins that have evolved to recognize protein modifications other than phosphorylation and hydroxylation. *N*-glycosylation acts as a targeting signal to eliminate intracellular glycoproteins by Fbx2-dependent ubiquitylation and subsequent proteasomal degradation.

N-glycosylation of the proteins occurs when newly synthesized proteins enter the endoplasmic reticulum (ER) through the translocation channel "translocon." *N*-glycans play an important role in glycoprotein transport and sorting (8), in particular at the initial step of secretion that occurs in the ER compartment (9, 10). *N*-linked glycoproteins are subjected to "quality control" in which aberrant proteins are distinguished from properly folded proteins and retained in the ER (10). The quality control system includes the calnexin-calreticulin cycle, a unique chaperone system that recognizes $Glc_1Man_{9-6}GlcNAc_2$ and assists refolding of misfolded or unfolded pro-

* This work was supported in part by Grants-in-Aid from the Ministry of Education, Science, and Culture of Japan and the Mizutani Foundation for Glycoscience, Tokyo, Japan. The costs of publication of this article were defrayed in part by the payment of page charges. This article must therefore be hereby marked "*advertisement*" in accordance with 18 U.S.C. Section 1734 solely to indicate this fact.

¶ To whom correspondence should be addressed: Laboratory of Frontier Science, Tokyo Metropolitan Inst. of Medical Science, 3-18-22 Honkomagome, Bunkyo-ku, Tokyo 113-8613, Japan. Tel.: 81-3-3823-2105; Fax: 81-3-3823-2965; E-mail: yyosida@rinshoken.or.jp.

[1] The abbreviations used are: E1, ubiquitin-activating enzyme; E2, ubiquitin-conjugating enzyme; E3, ubiquitin-protein ligase; chitobiose, di-*N*-acetylchitobiose; ConA, concanavalin A; WGA, wheat germ agglutinin; ER, endoplasmic reticulum; ERAD, ER-associated degradation; GST, glutathione *S*-transferase; GTF, GlcNAc-terminated fetuin; HA, hemagglutinin A; RCA, *Ricinus communis*; SCF, Skp1-Cullin1-F-box protein-Roc1; siRNA, small interfering RNA; TBS, Tris-buffered saline; TCRα; T-cell receptor α-subunit; UGGT, UDP-glucose:glycoprotein glucosyltransferase.

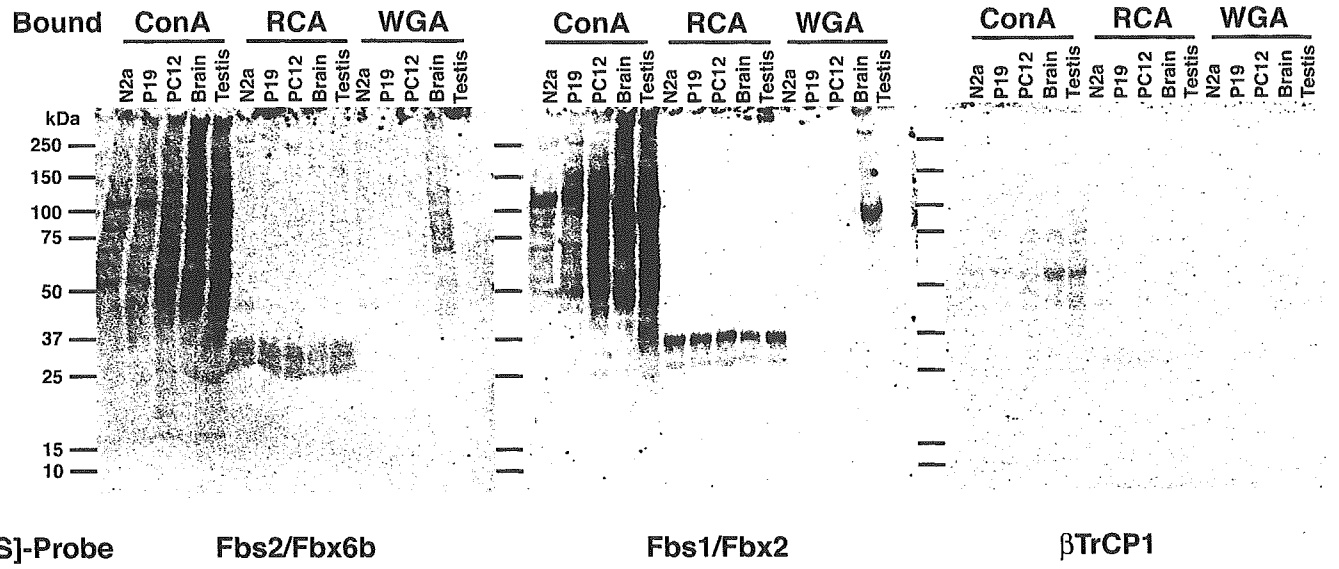

FIG. 1. **Interaction of Fbs2 and Fbs1 with endogenous glycoproteins containing *N*-linked high mannose type oligosaccharides.** Each extract of Neuro2a (*N2a*), P19, PC12 cells, and tissues from adult mice (brain and testis) was incubated with ConA, RCA, or WGA lectin-agarose. The lectin-bound proteins were separated with 4–20% SDS-PAGE and then transferred to membranes that were used for the overlay assay. ^{35}S-labeled Fbs2/Fbx6b ΔF, Fbs1/Fbx2 ΔN-2, and βTrCP1 ΔF were used for the probes.

teins. When the improperly folded or incompletely assembled proteins fail to restore their functional states, they are degraded by the ER-associated degradation (ERAD) system, which involves a retrograde transfer of proteins from the ER to the cytosol followed by degradation by the proteasome (11–13). Precisely how they are selected for ERAD remains unclear, but what is clear is that the trimming of *N*-glycans plays a key role in the selection process. Recent studies have demonstrated that $Man_8GlcNAc_2$ structures serve as part of the signal needed for ERAD and that a lectin for $Man_8GlcNAc_2$ in ER accelerates the turnover rate of the misfolded glycoprotein (14–16). It has been reported that many E3s are involved in the ERAD pathway, such as ER-embedded Hrd1 (17) and Doa10 (18), which have overlapping functions in yeast, and gp78 (19), CHIP (20) and Parkin (21), which ubiquitylate ER membrane proteins such as cystic fibrosis transmembrane conductance regulator (CFTR) and the Pael receptor in mammals. In addition, we have recently identified a novel member of the ERAD-linked E3 family, SCF^{Fbx2}, which participates in ERAD for selective elimination of glycoproteins (7). Misfolding or misassembly might be the general feature of all substrates; however, Fbx2 is expressed mainly in neuronal cells in the adult brain (22). Winston *et al.* (3) and Ilyin *et al.* (23) reported previously that several F-box proteins, including Fbx2, contain a conserved motif F-box-associated (FBA) domain or G-domain (sharing similarity with bacterial protein ApaG) in their C termini.

The present study is an extension of the above mentioned research work and was designed to determine whether these F-box proteins also recognize *N*-glycans. Our results showed that Fbx6b/FBG2 bound several glycoproteins, but other F-box proteins failed to bind any of the glycoproteins tested so far. In considering the results of these functional studies, we renamed Fbx2/FBG1 and Fbx6b/FBG2 Fbs1 (F-box protein that recognizes sugar chains 1) and Fbs2, respectively. We found that Fbs2 is widely distributed in a variety of mouse tissues, differing from the restricted expression of Fbs1. Furthermore, a dominant negative Fbs2 mutant suppressed degradation of a typical ERAD substrate, the T cell receptor α subunit (TCRα). Taken together, we concluded that Fbs2 is a new member of the E3-Fbs subfamily for ubiquitylation of *N*-linked glycoproteins and plays a role in the ERAD pathway.

EXPERIMENTAL PROCEDURES

Materials—Ribonuclease B, fetuin, asialofetuin type II, and thyroglobulin were purchased from Sigma. β-galactosidase (*Streptococcus* 6646K) and β-*N*-acetylhexosaminidase (Jack Bean) were purchased from Seikagaku-Kogyo (Tokyo, Japan), and *N*-glycosidase F was from Roche Applied Science. Affi-Gel 10 and 15 were from Bio-Rad and were used according to the instructions provided by the manufacturer. Di-*N*-acetylchitobiose (chitobiose) was purchased from Seikagaku-Kogyo, $Man_8GlcNAc_2$ was from Glyko (Upper Heyford, UK), $Man_5GlcNAc_1$ was from IsoSep AB, $GlcNAc_3Man_3GlcNAc_2$ (asialo-, agalacto-, tri-antennary complex) and $GlcNAc_2Man_3GlcNAc_2(Fuc_1)$ (asialo-, agalacto-, core-fucosylated bi-antennary complex) were from Ludger (Oxford, UK), and $Man_3GlcNAc_2$, $Man_5GlcNAc_2$, and $Man_5GlcNAc_2$-Asn were purchased from Sigma. $Man_9GlcNAc_2$ was a kind gift from Y. Ito. ConA, RCA, and WGA lectin-agaroses were purchased from Seikagaku-Kogyo.

Isolation of cDNAs Coding for F-box Proteins and Plasmid Construction—The sequences of mouse Fbs2/Fbx6b/FBG2 (accession number AF176526), Fbx17/FBG4 (accession number AF176532), and FBG3 (accession number XM_204068) cDNAs were obtained from the GenBank™ data base. The cDNAs for mouse Fbs2, Fbx17, and FBG3 were amplified by PCR with *Taq* polymerase (Sigma) from mouse kidney cDNA. The PCR primers were as follows: 5′-TCT CTG GGA TCC CCA TGG TCC ACA TCA AGG AG-3′ and 5′-GAG CCT GAG CGG CCG CTA ACG CCT TAG CCT TTG CCA-3′ for Fbs2; 5′-CTG ACC GGA TCC TCA TGG GAG CGC GGC CCT CG-3′ and 5′-ACC TGA AGG CGG CCG CAT CAC ATC ATG GTA GTC C-3′ for Fbx17; and 5′-ACG CCA GGA TCC CAG TAG GCA ACA TCA ACG-3′ and 5′-TGA GGA CTG CGG CCG CTC AGG AGG CAT CAG GGC AG-3′ for FBG3. PCR products were digested with *Bam*HI/*Not*I, subcloned into pBluescriptII SK+, and sequenced. The cDNAs of wild-type or deletion mutants were amplified by PCR with appropriate primers and ligated into *Bam*HI/*Not*I-cut pcDNA3-FLAG or pVL1393-His expression vector. The coding residues of the Fbs2 deletion mutant ΔF were from amino acids 47 to 295.

Overlay Assay—Cultured cells and mouse tissues were homogenized in 10 volumes of TBS (20 mM Tris-HCl, pH 7.5, and 150 mM NaCl) containing 0.5% Nonidet P-40 and protease inhibitor mixture (complete EDTA-free; Roche Applied Science). After centrifugation of the homogenate at 15,000 × *g* for 30 min, each supernatant (15-mg proteins) was incubated with 50 μl of various lectin-agaroses under gentle rotation at 4 °C for 2 h. The agaroses were washed with ice-cold TBS containing 0.5% Nonidet P-40, and bound proteins were boiled with SDS sample buffer. Proteins were separated with SDS-PAGE and blotted onto a membrane (Immobilon, Millipore, Bedford, MA). To prepare the [^{35}S]methionine-Fbs1 and Fbs2 probes, we constructed Fbs1-Metx3 and Fbs2-Metx3 plasmids for Fbs1 (ΔN-2) (7) and Fbs2 (ΔF), respectively, with three additional methionines at the C termini by subcloning them into pcDNA3-FLAG. The TNT Coupled Reticulocyte Lysate System

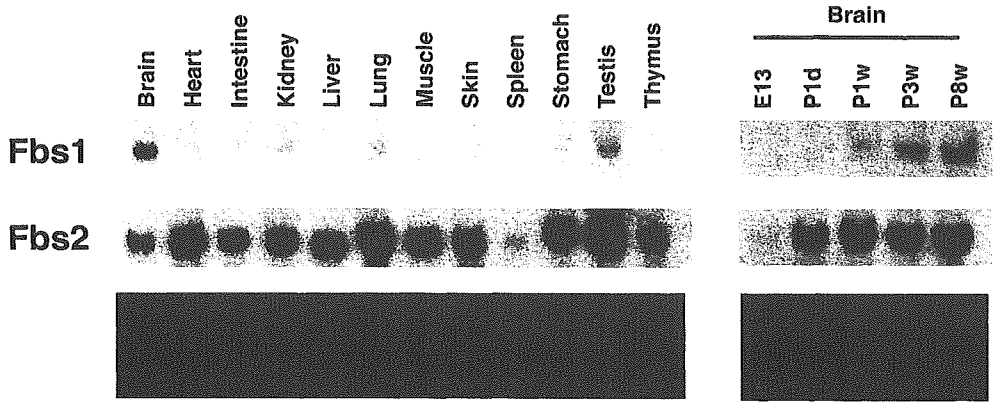

FIG. 2. **Expression of Fbs genes in mouse tissues.** Total RNA was extracted from adult mouse tissues or mice brains at different stages of development. A membrane preloaded with 15 μg of total RNA per lane was hybridized with radiolabeled mouse Fbs1 and Fbs2 cDNAs.

(Promega, Madison, WI) was used for generating [^{35}S]methionine-Fbs1, Fbs2, and βTrCP1. Membranes were blocked by 5% skim milk in TBS, washed, and then incubated with probes in 1% skim milk at 4 °C for 18 h with gentle shaking. Membranes were washed with TBS containing 0.05% Tween 20, air-dried, and analyzed by autoradiography.

Northern Blot Analyses—Tissues from 8-week-old ICR mice were employed for RNA extraction using the guanidine thiocyanate method. 15 μg of total RNA was fractionated on a denaturing formaldehyde-agarose gel (1%) and then transferred onto a nylon membrane (Nytran, Schleicher & Schuell). Northern blots were probed with the full-length Fbs1 or Fbs2 cDNA that had been labeled with [α^{32}P]dCTP. The blots were washed at 65 °C in 0.2× standard saline citrate containing 0.1% SDS and then exposed and analyzed with a Molecular Imager FX (Bio-Rad).

In Vitro Ubiquitylation Assays—Recombinant His-Ubc4 and His-Ubc12, His-NEDD8, and GST-ubiquitin were produced in *Escherichia coli*. Recombinant His-E1 (Uba1), His-APP-BP1/T7-Uba3, and SCF^{Fbs2} (FLAG-Skp1/Cul1-HA/His-Fbs2/T7-Roc1) were produced by baculovirus-infected HiFive or Sf9 insect cells. The SCF^{Fbs2} complex was obtained by simultaneously infecting four baculoviruses. These proteins were affinity-purified by a HiTrap HP column (Amersham Biosciences) as described previously (24).

The methods for preparation of GlcNAc-terminated fetuin (GTF) and deglycosylated fetuin (DGF) were described previously (7). One microgram each of GTF or DGF was incubated in 50 μl of the reaction mixture containing the ATP-regenerating system, 0.5 μg E1, 1 μg of Ubc4 (E2), 2 μg of SCF^{Fbs2}, and 6.5 μg of recombinant GST-ubiquitin in the presence or absence of the NEDD8 system (24) consisting of NEDD8 (10 μg), APP-BP1/T7-Uba3 (0.5 μg), and Ubc12 (0.5 μg) at 30 °C. After terminating the reaction by the addition of 25 μl of 3× SDS-PAGE sample buffer, the proteins in 8 μl of the boiled supernatants were separated with 4–20% SDS-PAGE, and the high molecular mass ubiquitylated proteins were detected by immunoblotting with an anti-fetuin (Chemicon) or anti-GST (Ab-1; Calbiochem, La Jolla, CA) antibody.

Pull-down Assay—Each 2.0 mg of glycoprotein was immobilized to 0.5 ml of Affi-Gel 10 or 15. Each cell extract prepared with TBS containing 0.5% Nonidet P-40 from FLAG-tagged Fbs2 (ΔF) or Fbs1 (ΔN-2)-expressing cells (25 μg) was incubated with 15 μl of various glycoprotein-immobilized beads, and bound proteins were eluted by boiling with SDS sample buffer or incubation with 15 μl of various concentrations of oligosaccharides at room temperature for 10 min. The eluates were separated by spin filtration.

RNA Interference Experiment—Twenty-one nucleotide dsRNAs were prepared by Dharmacon (Lafayette, CO). The siRNA sequences targeting Fbs2 mRNA (GenBank^{TM} accession number NM 018438) corresponded to the coding regions 285–304 (GAGGAUAUGUUUGCAUGGC) and 754–773 (ACAGCAGCAUUGUCGUCAG) relative to the first nucleotide of the start codon. A nonspecific control duplex was purchased from Dharmacon. 293T cells were transfected with siRNA and/or plasmid DNA by the use of LipofectAMINE Plus (Invitrogen). Total RNA was isolated with TRIZOL reagent (Invitrogen). Reverse transcription PCR was performed using total RNA of 293T cells as a template. The 5′ and 3′ primers were 5′-CCTCCTGGCGGGACCTCATCG-3′ and 5′-ACCAGCTGGGACTTGAGGCAC-3′ for Fbs2 and 5′-GAGCTGAACGGGAAGCTCAC-3′ and 5′-ACCACCCTGTTGCTGTAGC-3′ for the glyceroaldehyde-3-phosphate dehydrogenase, respectively.

Metabolic Labeling and Immunoprecipitation—293T cells were transiently transfected with1 μg of the TCRα-HA expression plasmid and 1 μg of the Fbs2 plasmid or pcDNA3. Twenty-four hours after transfection, 293T cells were starved for 30 min in methionine- and cysteine-free Dulbecco's modified Eagle's medium containing 10% dialyzed fetal calf serum. Cells were then labeled for 30 min with 150 μCi of Pro-Mix L-^{35}S *in vitro* cell-labeling mix (Amersham Biosciences) per milliliter. For pulse-chase experiments, cells were washed after labeling and chased with complete Dulbecco's modified Eagle's medium containing 10% fetal calf serum for different lengths of time at 37 °C. In experiments with tunicamycin, cells were treated with 5 μM tunicamycin (Wako Pure Chemical Industries, Osaka, Japan) 2 h prior to and throughout the labeling period. In the experiments of Fbs2 knock-down by siRNA, cells that had been co-transfected with 4.2 μg (300 pmol) of siRNA duplex and 1 μg of the TCRα-HA expression plasmid and cultured for 48 h were metabolically labeled with the cell-labeling mix. After labeling or chase, cells were washed with ice-cold phosphate-buffered saline and lysed with TBS buffer containing 0.1% SDS and 1% Nonidet P-40. In co-immunoprecipitation experiments, TBS buffer containing 1% Triton X-100 was used for lysing. After one cycle of freeze-thaw, cell lysates were cleared by centrifugation, and the supernatants were used for immunoprecipitation. Briefly, the supernatants were precleared with protein A-Sepharose (Amersham Biosciences), mouse monoclonal antibodies, anti-FLAG (M2; Sigma), and anti-HA (HA11, BABCO) were then added, and incubation was performed at 4 °C with rotation. Immune complexes were then incubated with protein A-Sepharose, collected by centrifugation, and washed four times with the lysis buffer. For protein analysis, immune complexes were dissociated by heating in SDS-PAGE sample buffer and loaded onto SDS-PAGE. After drying, gels were exposed, and radioactive band intensity was measured using Molecular Imager FX. All experiments described in this study were approved by the institutional ethics review committee for animal experimentation.

RESULTS

Fbs2 Interacts with High Mannose Oligosaccharide-containing Glycoproteins—We reported recently that Fbs1/Fbx2/NFB42 forms a SCF^{Fbs1} ubiquitin ligase complex that targets *N*-linked high mannose oligosaccharides in glycoproteins for ubiquitylation (7). Fbs1 interacts with substrate glycoproteins through its C-terminal domain, which shows high homology with other F-box proteins (3, 23). To explore the presence of other F-box proteins that recognize *N*-glycans, we isolated mouse cDNA clones that encode F-box proteins homologous to Fbs1 and examined the properties of the proteins with regard to interaction with *N*-linked glycoproteins. The mouse Fbs2/Fbx6b/FBG2, Fbx17/FBG4, and FBG3 cDNA clones obtained by reverse transcription PCR were expressed in 293T cells as FLAG-tagged, full-length F-box proteins, and these cell extracts were incubated with various *N*-linked glycoproteins. Only Fbs2 bound several glycoproteins, whereas the other F-box proteins failed to bind any of the glycoproteins tested (see Fig. 3, and data not shown).

Next, we investigated the interaction of these F-box proteins with oligosaccharides on endogenous proteins by overlay assay. To enrich glycoproteins that were fractionated by their oligo-

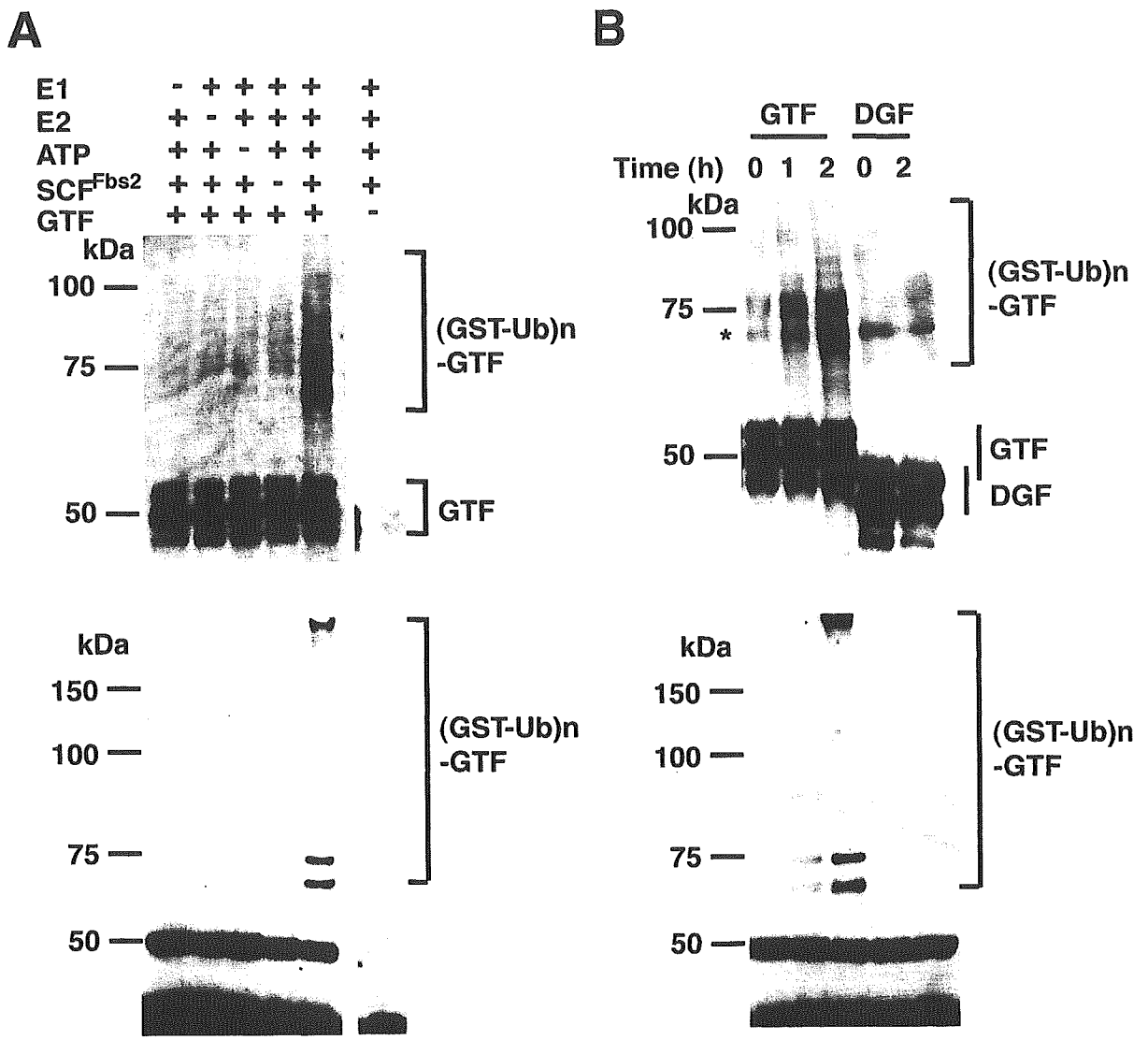

FIG. 3. **SCF^{Fbs2} complex ubiquitylates the *N*-glycosylated substrate *in vitro*.** *A*, *in vitro* ubiquitylation of GTF by the SCF^{Fbs2} E3-ligase system. Ubiquitylation of GTF was confirmed by omission of E1, E2, ATP, E3, or GTF from the reaction mixtures at 30 °C for 2 h. The higher molecular mass-ubiquitylated GTF ((GST-Ub)n-GTF) was detected by immunoblotting with anti-fetuin (*top*) and anti-GST (*bottom*) antibodies. *B*, *N*-linked oligosaccharides are required for ubiquitylation. *In vitro* ubiquitylation was performed with GTF and DGF. *Asterisk*, a nonspecific band detected by anti-fetuin antibody.

saccharide structures, we prepared proteins bound to lectins from the extracts of several cell lines and adult mouse tissues. These glycoproteins were then separated by SDS-PAGE and detected by each ^{35}S-labeled F-box protein. In glycoproteins bound to ConA, a lectin that binds to high mannose oligosaccharides, many protein bands were detected by Fbs1 and Fbs2 probes (Fig. 1). These glycoproteins did not bind to βTrCP1, which is a F-box protein with WD repeats for substrate recognition (1, 2) (Fig. 1). On the other hand, a few proteins reacted with Fbs1 and Fbs2 in the glycoproteins bound to RCA120, a lectin that binds to terminal Galβ1–4GlcNAc or WGA and is specific for terminal GlcNAc or sialic acids (Fig. 1). The broad 75–80-kDa protein band(s) and the 60-kDa protein in the WGA-bound fraction prepared from brain extract seemed to be identical to that bound to ConA. Because many proteins contain several and/or structurally diversified oligosaccharides, these 75–80-kDa and 60-kDa proteins may be modified by high mannose oligosaccharides and complex type glycans. The whole pattern of the protein bands detected by the Fbs2 probe was almost the same as those detected by Fbs1, but the strength of binding activity with Fbs2 seemed to be somewhat weak compared with Fbs1. Any glycoproteins concentrated with ConA, RCA120, and WGA lectins failed to be detected with Fbx17 and FBG3 probes (data not shown). These results suggest that high mannose oligosaccharides are important for the substrate recognition by Fbs2 as well as Fbs1.

Expression of Fbs Genes in Mouse Tissues—Fbs1 is reported to be expressed in the adult rat brain but not in non-neural tissues (22). We compared the expression patterns of Fbs1 and Fbs2 by Northern blot analysis in 12 different mouse tissues. This analysis demonstrated that the Fbs1 transcript of ~1.5 kb mRNA was expressed in the brain and, to a lesser extent, in the testis (Fig. 2). Western blot analysis using Fbs1 polyclonal antiserums confirmed that Fbs1 protein is present only in the brain and testis among the 12 different tissues examined (data not shown). The transcription of Fbs1 appeared in 1-week-old mice, reaching the highest level in the adult brain. On the other hand, an ~1.8-kb transcript of Fbs2 was detected in various tissues, mainly in the heart, intestine, kidney, liver, lung, muscle, stomach, and testis as well as other tissues (brain, skin, spleen, and thymus) with low abundance. Fbs2 expression was not observed in the fetus, but became detectable after birth and increased in the adult brain. Thus, although the

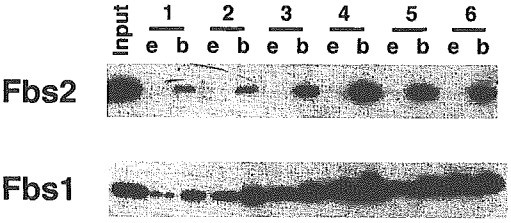

FIG. 4. **Pull-down analysis of the interaction of Fbs proteins with *N*-glycoproteins.** Extracts of cells expressing Fbs2 ΔF and Fbs1 ΔN-2 were incubated with glycoprotein-immobilized beads. The beads were washed, and then halves of the beads were eluted with *N,N'*-diacetylchitobiose (*e*), and the other halves were boiled with sample buffer (*b*). Lysates (7.5 μg), eluates, and bound proteins were analyzed by immunoblotting an anti-FLAG antibody (*top*) and their binding efficiencies were classified as −, ±, +, ++, and +++ (*bottom*).

Proteins (*N*-Glycan)	Fbs2		Fbs1	
	elute	bound	elute	bound
1. Fetuin (tri-antennary complex)	-	±	±	+
2. Asialo Fetuin (Gal-terminal tri-antennary)	-	±	+	++
3. GTF (GlcNAc-terminal tri-antennary)	-	+	+	++
4. Man-terminated Fetuin ($Man_3GlcNAc_2$)	-	++	+++	+++
5. Thyroglobulin ($Man_{7\text{-}9}GlcNAc_2$)	-	++	+	+++
6. RNaseB ($Man_{5\text{-}7}GlcNAc_2$)	-	++	++	+++

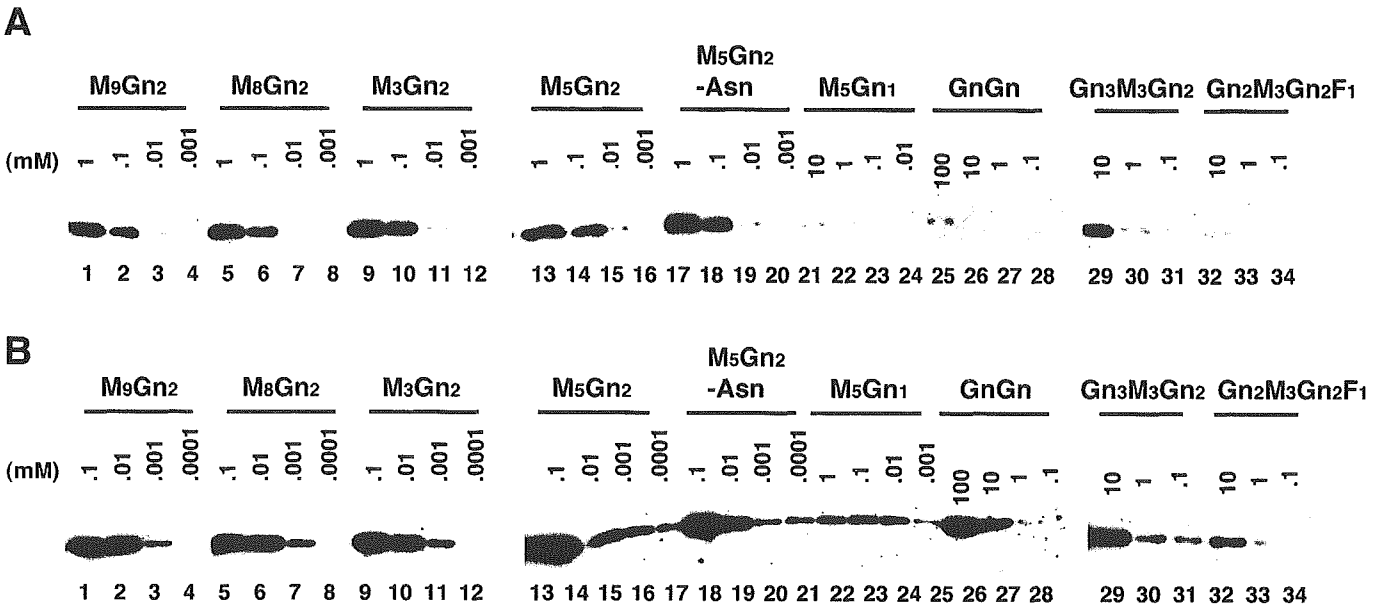

FIG. 5. **Elution of Fbs proteins bound to RNase-B immobilized beads with oligosaccharides.** After Fbs2 ΔF (*A*) or Fbs1 ΔN-2 (*B*) was retained on the RNase B immobilized beads, the bound Fbs protein was eluted by incubation with various concentrations of $Man_9GlcNAc_2$ (M_9Gn_2), $Man_8GlcNAc_2$ (M_8Gn_2), $Man_3GlcNAc_2$ (M_3Gn_2), $Man_5GlcNAc_2$ (M_5Gn_2), $Man_5GlcNAc_2$-asparagine (M_5Gn_2-*Asn*), $Man_5GlcNAc_1$ (M_5Gn_1), *N, N'*-diacetylchitobiose (*GnGn*), $GlcNAc_3Man_3GlcNAc_2$ ($Gn_3M_3Gn_2$), or $GlcNAc_2Man_3GlcNAc_2$(Fuc) ($Gn_2M_3Gn_2F_1$). Note the differences in the concentrations of high mannose type oligosaccharides for elution between Fbs2 and Fbs1.

expression of Fbs1 is restricted to the brain and testis, the Fbs2 transcript is ubiquitously expressed in all tissues examined.

In Vitro Ubiquitylation Assay of Fbs2—To directly demonstrate the E3 ubiquitin ligase activity in SCF^{Fbs2}, we devised a fully reconstituted system for ubiquitylation of GTF in the presence of the NEDD8 system. To this end, we produced all components required for these systems as recombinant or purified proteins (see "Experimental Procedures"). Ubiquitylation of GTF by GST-tagged ubiquitin was detected by immunoblotting using an anti-fetuin or anti-GST antibody. No ubiquitylation activity was detected in the absence of E1, E2, ATP, SCF^{Fbs2}, or GTF (Fig. 3*A*). The amount of ubiquitylation increased in a time-dependent manner (Fig. 3*B*). In addition, *N*-glycanase F-treated fetuin (DGF) was not ubiquitylated *in vitro* by SCF^{Fbs2} (Fig. 3*B*). These results indicate that SCF^{Fbs2} is an E3 ubiquitin ligase that recognizes *N*-glycans in glycoproteins.

Binding Specificities of N-Glycans to Fbs1 and Fbs2—To compare the binding specificities to *N*-glycans between Fbs1 and Fbs2, a pull-down assay using several *N*-linked glycoproteins was carried out (Fig. 4). Whereas Fbs2 could bind to GTF but weakly to fetuin and asialofetuin, Fbs1 bound to asialofetuin and GTF more efficiently than to intact fetuin. Both Fbs1 and Fbs2 bound efficiently with glycoproteins containing mannose-terminated *N*-glycan(s), mannose-terminated fetuin, thyroglobulin, and RNase B, suggesting that mannose-terminated *N*-glycans (the number of mannose residues is irrelative) are required for the efficient binding of these Fbs proteins. On the other hand, the efficiency of elution of the proteins from the glycoproteins by chitobiose was different between Fbs1 and Fbs2. Although Fbs1 could be eluted efficiently by 0.1 M chitobiose from the *N*-linked glycoproteins tested, Fbs2 failed to be eluted by chitobiose. To characterize in more detail the binding specificities, we first quantified the oligosaccharide binding to Fbs proteins using a series of oligosaccharides labeled with 2-aminopyridine (25). However, we found that the innermost GlcNAc residue modified with 2-aminopyridine greatly reduced ($10^{2\text{-}3}$) the Fbs1 and Fbs2 binding (data not shown). Therefore, we next examined the efficiency of elution of the Fbs proteins

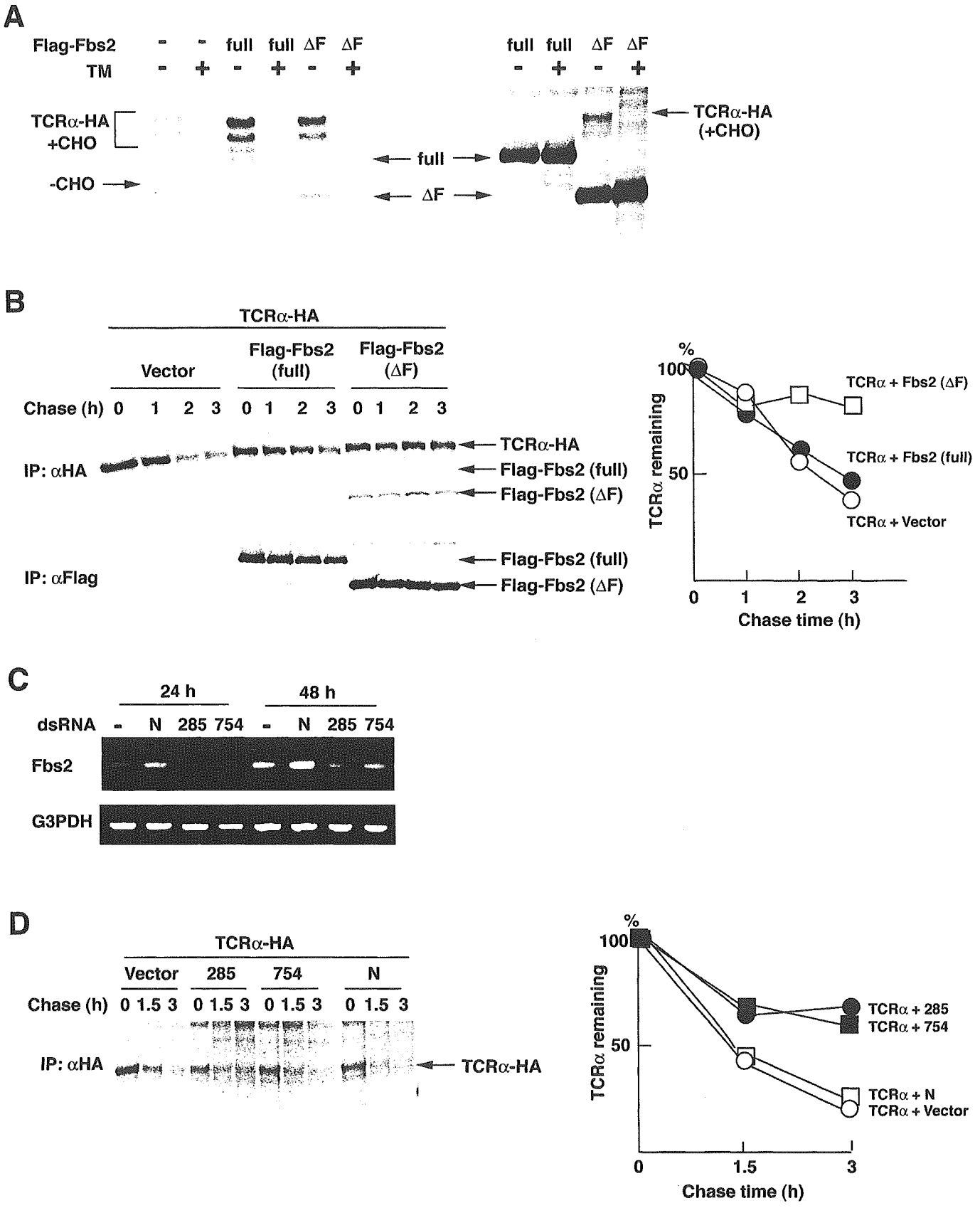

FIG. 6. **Involvement of Fbs2 in the ERAD pathway.** *A*, interaction between TCRα-HA and wild-type or truncated forms of Fbs2. 293T cells were transfected with TCRα-HA and/or various Fbs2 constructs. Twenty-four hours after transfection, cells were treated with (+) or without (−) 5 μg/ml tunicamycin (*TM*) for 2 h. Then, cells were labeled with [^{35}S]Met/Cys in the absence or presence of tunicamycin for 30 min. TCRα and Fbs2 derivatives were immunoprecipitated by anti-HA and anti-FLAG antibodies, respectively. *CHO*, carbohydrate oligosaccharide. *B*, effect of Fbs2 on the stability of TCRα. TCRα-HA was co-transfected with an empty vector (*Vector*), wild type (*full*), or FLAG-Fbs2 ΔF. 293T cells were pulse-labeled with [^{35}S]Met/Cys and chased for the indicated times. TCRα and Fbs2 derivatives were immunoprecipitated (*IP*) by anti-HA and anti-FLAG antibodies, respectively. The plotted data provide quantification analysis of the stability of TCRα over time. *C*, effect of nonspecific (*N*) or